Monopole excitations and $E0$ transitions in even–even nuclei

N. A. Voinova-Eliseeva and I. A. Mitropol'skiĭ

B. P. Konstantinov Leningrad Institute of Nuclear Physics, Leningrad

Fiz. Elem. Chastits At. Yadra **17**, 1173–1230 (November–December 1986)

The existing theoretical ideas about the structure and properties of nuclear monopole states and $E0$ transitions are analyzed on the basis of the most recent compilation of experimental data. The main modes forming not only the low-lying 0^+ states but also giant monopole resonances are identified in light, magic, spherical, deformed, and transitional even–even nuclei. Typical results are given of calculations obtained in collective and microscopic models, as well as results based on qualitative considerations about the nature of these states deduced from their systematic behavior. The intensity of $E0$ transitions is characterized by "single-particle" estimates and energy-weighted sum rules. Particular attention is devoted to anomalies that are manifested in the decay properties of the monopole states and to their physical interpretation. The results of a self-consistent approach to pairing correlations in nuclei are presented in detail. The possibility of experimental investigation of monopole states excited by the decay of a bound muon is discussed.

INTRODUCTION

There have been many experimental and theoretical studies of monopole states (spin–parity $I^\pi = 0^+$) and $E0$ transitions in nuclei. Various aspects of this problem have been considered in a number of reviews.[1–7] The particular interest in nuclear monopole excitations arises because the structure of the 0^+ states is distinguished by great complexity and a variety of forms of the effective nuclear interaction involved in their formation. Indeed, in many even–even nuclei several 0^+ levels (sometimes up to five) are found below the energy gap ($E \lesssim 2$ MeV). This indicates that these levels have a different nature and interact weakly with one another. For otherwise the residual interaction would lead to repulsion between them.

The simple listing of the experimental methods used in their excitation is an indication of the variety in the nature of monopole levels in nuclei. As a rule, 0^+ levels of similar energies in a given nucleus cannot be excited by one and the same reaction, and this also indicates significant differences in their structures. The most information about monopole states is provided by radioactive decay, the (p, p') reaction, double Coulomb excitation, reactions involving light ions, and also the reactions (p,t) and $(^3\mathrm{He},n)$ and their inverse reactions, the $(^6\mathrm{Li},d)$, $(\alpha,2n)$, $(p,2n)$, (n,γ) reactions, and so forth. The first three methods of exciting nuclei serve to study the electromagnetic decay of low-lying 0^+ states. Giant monopole resonances are excited in inelastic scattering of electrons, hadrons, and α particles. Reactions involving the transfer of a pair of particles are helpful for investigating the pairing component of the wave function. The remaining reactions give more or less fortuitous information about monopole nuclear states.

The aim of the present review is to give, as far as possible, a unified picture of the ideas and methods underlying the various model approaches to the problem of monopole excitations in nuclei. Historically, nuclear models developed following two limiting concepts: independent-particle models, which deal with single-particle motion, and continuum models, which absolutize the collective forms of the motion. Accordingly, the nuclear models can be divided into two groups—the microscopic models and the collective or macroscopic models. Usually, theoretical reviews are based on a classification of the existing nuclear models, the experimental data being used to illustrate their achievements and difficulties. The shortcoming of such an approach is that the exposition is necessarily fragmentary, reflecting the objective state of the theory. In such a situation, it is more natural, in our view, to present essentially the same material on the basis of the observed properties of nuclei, taking one or other model to describe them as appropriate.

Depending on their properties, nuclei can be divided into large groups: light nuclei, magic nuclei and nuclei with closed shells, spherical nuclei, deformed nuclei, and transitional nuclei. Within each group, the properties of the monopole excitations are qualitatively similar, and this makes it possible to identify typical features and describe them by means of definite models. On the transition from one group of nuclei to another, or from certain properties to others (for example, the excitation energies), the model representations also change. This interdependence of the models and properties of nuclei is taken as the basis of the present review.

Its material is accordingly arranged as follows. In the first section, we discuss the general properties of electric monopole transitions. Then comes a description of characteristic monopole states and transitions in light nuclei. The following section is devoted to the properties of low-lying 0^+ states in magic nuclei and closed-shell nuclei. In a separate section, we discuss the properties of giant monopole resonances observed in these nuclei. We then consider the properties of collective monopole excitations in spherical and deformed nuclei in the framework of the vibration model. The following section of the review is devoted to the interaction of the elementary modes that leads to anharmonicity in the spectra of the transitional nuclei. We then discuss the main results of the microscopic description of the structure

 0090-4759/86/060521-28$04.40

of low-lying 0^+ states in the superfluid nuclear model with self-consistent pairing. The possibilities of the new method of monopole excitation of nuclei through the decay of a bound muon in a mesic atom are discussed in the final section of the review. At the end, we give the main conclusions relating to the theoretical description of 0^+ states and $E0$ transitions in even–even nuclei.

The main attention in the review is devoted to the description of monopole excitations in nuclear models without a detailed description of these models themselves or of the results of their application to other types of excitation. Except where stated otherwise, details can be found in the well-known monographs of Refs. 8–10 on nuclear physics. All the experimental data on 0^+ states and $E0$ transitions in even–even nuclei used in the text, tables, and figures are taken from the compilation of Ref. 11, which collects together the information available up to the middle of 1985. Tables of estimated experimental data are given in the Appendix.

ELECTRIC MONOPOLE TRANSITIONS

Electromagnetic transitions are extremely important for understanding the nature of the various modes of nuclear monopole excitations and analyzing them. Monopole transitions of electric type occupy a distinguished position among the electromagnetic transitions. They are associated with interesting and rather poorly studied aspects of nuclear structure such as the changes in the rms charge radii, the isotopic and isomer shifts, the compressibility of nuclear matter, radial oscillations of the density, breathing modes, etc.

The main factor giving rise to $E0$ transitions is the Coulomb interaction of the nuclear nucleons with electrons of an atomic shell or the Dirac background. Residual interactions, electromagnetic or other, usually play no part.[1] Single-photon $E0$ transitions are strictly forbidden by angular-momentum conservation. The $E0$-transition probability

$$w(E0) = w_e(E0) + w_p(E0) + w_{\gamma\gamma}(E0) \tag{1}$$

is made up of the probabilities w_e and w_p of electron and pair conversion and the probability $w_{\gamma\gamma}$ of a two-photon transition. This last term refers to processes of higher order, and usually $w_{\gamma\gamma} \ll w_{e,p}$. For example, for the mixed two-photon $(2E1 + 2M1)$ transition from the first excited 0^+ state to the ground state in the ^{40}Ca and ^{90}Zr nuclei the ratio $w_{\gamma\gamma}/w(E0)$ is $4.5(10)\cdot 10^{-4}$ and $1.8(2)\cdot 10^{-4}$, respectively.[12]

Pair conversion is a threshold process and occurs only at transition energies exceeding two electron masses. The probabilities of electron and pair conversion[13]

$$w_{e,p}(E0) = \rho^2(E0)\,\Omega_{e,p} \tag{2}$$

are proportional to the square of the dimensionless matrix element

$$\rho(E0;\ i \to f) = \langle f \mid M(E0) \mid i\rangle / eR_0^2, \tag{3}$$

which carries information about the nuclear structure. Here, $R_0 = r_0 A^{1/3}$ is the charge radius of the nucleus, and $\Omega_{e,p}$ are electron factors, which depend on the charge Z of the nucleus and on the transition energy E and can be calculated independently of the nuclear structure.[1,6,14] The monopole-transition operator

$$M(E0) = e\sum_{p=1}^{Z} r_p^2 \tag{4}$$

acts only on the protons, although neutrons are sometimes taken into account with effective charges.

Besides the energy, the matrix element $\rho(E0)$ is the main characteristic of a nuclear monopole transition that can be extracted from experiments. As a rule, monopole transitions are accompanied by more intense quadrupole transitions. In the cases when the lifetime of the investigated level cannot be determined, one measures the $E0/E2$ mixing[15]:

$$X(E0/E2) = \frac{e^2R_0^4\rho^2(E0;\ i \to f)}{B(E2;\ i \to f')}. \tag{5}$$

The states i and f must have the same spins and parity. For transitions between monopole states, $E2$ transitions from a given 0^+ level to the 2^+ level nearest the final state are considered. The experimental information about a transition is often restricted to the value of precisely this parameter. On the other hand, since the ratio $X(E0/E2)$ does not depend on the electron factors or on the transition energies, it is helpful in comparisons with nuclear models.

The simplest qualitative estimate for the matrix element, $\rho(E0) = 1$,[13] corresponds to a transition with completely overlapping wave functions of the initial and final states. It does not contain a dependence on the mass number A and greatly exceeds the observed values even in light nuclei. In the single-particle model, $E0$ transitions within one shell are forbidden. Low-energy $E0$ transitions arise only through correlations.[8] If the 0^+ states have two-proton configurations,

$$\left.\begin{aligned} |0_i^+\rangle &= a|j_1^2(0^+)\rangle + b|j_2^2(0^+)\rangle;\\ |0_f^+\rangle &= -b|j_1^2(0^+)\rangle + a|j_2^2(0^+)\rangle, \end{aligned}\right\} \tag{6}$$

then the matrix element of the $E0$ transition between them is proportional to the change in the mean-square charge radius:

$$\rho(E0;\ 0_i^+ - 0_f^+) = 2ab(\langle r^2\rangle_f - \langle r^2\rangle_i)/R_0^2. \tag{7}$$

We note that the connection between $\rho(E0)$ and the change in the charge radius still holds for more complicated configurations. In the oscillator approximation, $\langle r^2\rangle_N = (N + 3/2)\hbar/m\omega_0$ and for (7) when $\Delta N = 1$ we can obtain a simple estimate by setting $a = b = 1/\sqrt{2}$ (maximal mixing of the states):

$$\rho_0(E0) = 0{,}70\,A^{-1/3}. \tag{8}$$

This is sometimes called the "single-particle estimate." Together with the single-particle probability of the $E2$ transition, $B_0(E2) = 5.94\cdot 10^{-2}A^{4/3}e^2\cdot\mathrm{F}^4$, it leads to an estimate of the mixing parameter:

$$X_0 = 17A^{-2/3}. \tag{9}$$

These estimates can be used as a scale for the analysis of experimental data.

To determine the degree of collectivization of the nuclear states and test the consistency of theoretical results, energy-weighted sum rules are helpful[8,16]:

$$m_k = \sum_n E_n^k |\langle n|M|0\rangle|^2, \tag{10}$$

where M is the operator of the transition from the ground state $|0\rangle$ to the excited states $|n\rangle$ with energies E_n, measured from the ground-state energy. On the right-hand side of (10), it is possible to go over to the expectation value with respect to the ground state. In particular, for $k = 1$

$$m_1 = \frac{1}{2}\langle 0|[M, [H, M]]|0\rangle, \tag{11}$$

where H is the Hamiltonian of the nucleus. This gives for the velocity-independent monopole-transition operator (4) the expression

$$m_1(E0) = 2\frac{\hbar^2}{m} e^2 Z \langle r^2\rangle, \tag{12}$$

where Z is the charge, and $\langle r^2\rangle$ is the mean-square radius of the nucleus. The connection with the global characteristics of the nucleus and the rather general assumptions about the nature of the Hamiltonian permit the designation of the sum rule (12) as model-independent.

In Table I, which is based on the available experimental data, we analyze the contributions $s_1^{(n)} = e^2 R_0^4 E_n \rho_n^2(E0)$ of the lowest monopole states of the ^{16}O nucleus to the sum rule (10). The expression (12) gives $m_1(E0) = 7020\ \text{MeV}^2 \cdot \text{F}^5$ for the experimental value $\langle r^2\rangle^{1/2} = 2.71$ F. It can be seen that even quite collectivized (according to the single-particle estimate (8), $\rho_0(E0) = 0.28$) low-lying 0^+ states make a small contribution to the sum rule. The giant monopole resonances are responsible for the main part of it.

Study of monopole transitions in nuclei permits conclusions about fine details of their structure. Particularly important in the given context is the investigation of the dependence of the reduced probability of $E0$ transitions on the excitation energy of the levels. With increasing energy, the structure of the monopole states changes qualitatively, and this can lead to significant changes in the decay characteristics. For example, for 0^+ levels in the region of the two-quasiparticle threshold we note (Fig. 1) a growth in $X(0^+) = B(E0; 0_n^+ - 0_1^+)/B(E2; 0_n^+ - 2_1^+)$ by two orders of magnitude and more compared with the value characteristic of the first excited 0^+ state.[17] Such an anomaly can serve as a qualitative test in the choice of definite models. The conclusion that it has a structural nature is supported by the appearance of a similar anomaly in other monopole transitions. In particular, an analogous maximum is observed in deformed nuclei for the ratio $X(2^+) = B(E0; 2_n^+ - 2_1^+)/B(E2; 2_n^+ - 2_1^+)$ (Fig. 1), where 2_n^+ are states of the rotational bands based on the excited 0_n^+ state and the ground 0_1^+ state, which have, as a rule, a similar structure.

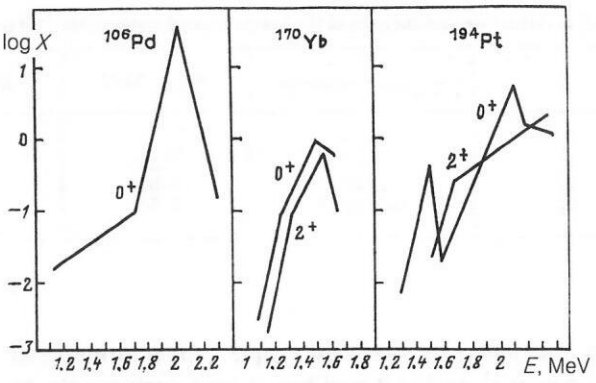

FIG. 1. Dependence of the ratio $X(E0/E2)$ for 0^+ and 2^+ levels on the excitation energy.

MONOPOLE EXCITATIONS IN LIGHT NUCLEI

In light nuclei ($A < 40$) with closed p and sd shells the effects of the saturation of the nuclear forces characteristic of heavier nuclei are absent. This governs the specific nature of the theoretical ideas used to describe their structure. In the first place, we must mention here the methods based on direct solution of the Schrödinger equation

$$\left\{-\frac{\hbar^2}{2m}\sum_{i=1}^{A}\Delta_i + \sum_{i<j}^{A} V_{ij} - E\right\}\Psi(1, 2, \ldots, A) = 0 \tag{13}$$

with an effective two-particle interaction V_{ij}.

The greatest number of results on the description of the structure of light nuclei has been obtained on the basis of the many-particle shell model. In it, the wave function and energy spectrum of the nucleus are determined by diagonalizing the Hamiltonian on a complete set of antisymmetrized single-particle functions. The correlations in the motion of the nucleons associated with the Pauli principle are taken into account automatically. Since in reality the set of basis functions is never complete, this approach is subject to the specific problem of the optimal choice of the representation, which must admit fairly rapid convergence and simultaneously a simple calculation of the matrix elements of the two-particle interaction.

TABLE I. Contributions of the lowest 0^+ states of the ^{16}O nucleus to the monopole sum rule.

$E(0_n^+)$, MeV	$\rho_n(E0)$	$s_1^{(n)}$, MeV$^2\cdot$F^5	$s_1^{(n)}/m_1(E0)$
6.05	0.41	220	0.031
12.1	0.48	602	0.086
14.0	0.41	509	0.073
Sum		1331	0.190

TABLE II. Structure and energies of the lowest excited states of the ^{20}O nucleus.[21]

I_n^π	Ground-state configuration	E_{theor}, MeV	E_{exp}, MeV
0_1^+	$(sd)^4$	0	0
2_1^+	$(sd)^4$	1.869	1.674
4_1^+	$(sd)^4$	3.620	3.570
0_2^+	$(sd)^6(p)^{-2}$	4.400	4.456

A restriction to relatively simple configurations and model potentials makes it possible, at least qualitatively, to describe the structure and position of the lowest nuclear levels in the many-particle shell model.[18–20] The excited 0^+ states always have a more complicated particle–hole configuration than the ground state and the neighboring states with nonzero spins. As a typical example we can take the interpretation of the lowest states of the ^{20}O nucleus[21] given in Table II.

The influence of three-particle forces on the position and structure of the low-lying levels in nuclei of the *sd* shell is small.[22] Their inclusion leads only to a certain repulsion of the levels, and this can be understood as due to allowance for the Pauli principle for valence nucleons. In the shell model, it is difficult to discuss the qualitative influence of the three-particle forces on the properties of the low-lying nuclear states on account of the effective nature of the two-particle interaction, the parameters of which are determined independently by fitting to experimental data and already contain contributions from the three-particle interaction.

The wave functions of the shell model (independent particles) take into account only the kinematic correlations in the motion of the nucleons associated with the Pauli principle and the symmetry of the state. The main difficulty in the case of light nuclei is the separation of the center-of-mass motion.[23] The method of K harmonics is free of this shortcoming.[24,25] Allowance for the collective degree of freedom associated with the relative motion of the nucleons makes it possible in this method to describe dynamical correlations that have no analog in the shell model. This made it possible to explain the structure of the ground states of light nuclei and reproduce the essential difference between the properties of the ground and excited 0^+ states. Table III gives the results of calculations of the energies, rms radii, and quadrupole moments of 0^+ levels in the ^{12}C and ^{16}O nuclei. In particular, the transition from a spherical or even oblate ($Q<0$) shape of the nucleus in the ground state to a prolate shape in the excited state can be described.[24] The calculated changes in the rms radii can be related to the monopole-transition matrix element (7), and they are found to agree well with the observed values of $\rho(E0)$. For monopole excitations with respect to the collective coordinate the method of K harmonics gives much more accurate wave functions in p-shell nuclei than does the shell model. The main contribution to the wave function of the excited 0^+ states of these nuclei derives from $4p4h$ configurations.

Figure 2 shows the schematics of the experimental values of the matrix element $\rho(E0)$ in light nuclei together with the single-particle estimate (8). Besides transitions that agree well with the simple particle–hole picture of 0^+ excitations, for which $\rho(E0)\approx\rho_0(E0)$, there are in light nuclei transitions that are significantly accelerated, $\rho(E0)>\rho_0(E0)$.

In light nuclei, $4p4h$ configurations can be introduced phenomenologically in the framework of the α-cluster model. It combines features of the single-particle and collective models and is based on the idea that, as a result of short-range correlations, the nucleons are combined into clusters, the relative motion of which determines the state of the nucleus. This model can be regarded as an extension of the shell model. The choice of several α-cluster states can give a better approximation to the correct nuclear wave functions than a large number of many-particle–hole configurations in shell calculations.[26] If a nuclear excitation is due to transition of a

TABLE III. Properties of the ground states and first excited 0^+ states in the ^{12}C and ^{16}O nuclei. The spread of the theoretical values is due to the choice of different two-particle potentials.

Parameter		^{12}C		^{16}O	
		0_1^+	0_2^+	0_1^+	0_2^+
$E(0^+)$, MeV	Theory	0	7.3—7.6	0	5.7—7.0
	Experiment	0	7.65	0	6.05
$\langle r^2\rangle^{1/2}$, F	Theory	2.6—2.7	3.4—3.5	2.7—2.8	3.2—3.3
	Experiment	2.42	—	2.71	—
Q, F^2	Theory	—(22—24)	105—110	0	79—81
	Experiment	—25.4	—	0	70.5
$\rho(E0)$	Theory	—	0.61—0.73	—	0.33—0.39
	Experiment	—	0.72 (2)	—	0.41 (1)

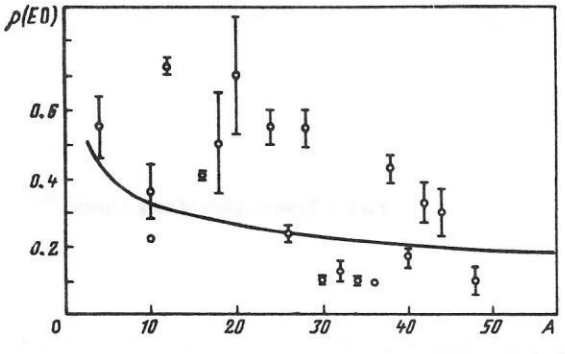

FIG. 2. Matrix elements $\rho(E0)$ in light nuclei.

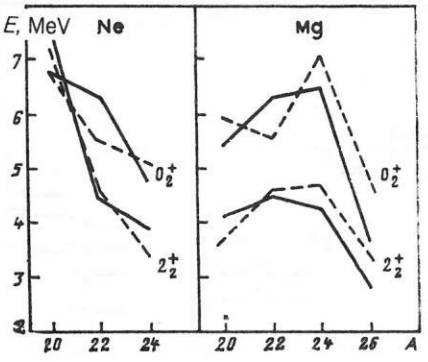

FIG. 3. Energies of 0_2^+ and 2_2^+ states in Ne and Mg isotopes.[32] The theoretical values are joined by the continuous lines, and the experimental points by the broken lines.

cluster to a higher level, then it can be characterized by a single-particle estimate taking into account the multiplicity of the cluster charge.

In the α-cluster nuclei (^{12}C, ^{16}O, ^{20}Ne, ^{24}Mg, ^{28}Si) the first 0^+ state corresponds to excitation of an α particle with respect to the core, and therefore the matrix element $\rho(E0)$ must be about twice the estimate (8), as can be seen from Fig. 2. With increasing excitation energy not only transitions of a cluster to higher levels but also core excitations become possible. Thus, the states of the ^{16}O nucleus can be regarded as excitations in the $\alpha + {}^{12}$C system[27] (Table IV). The 11.26-MeV level corresponds to a two-quantum excitation of an α cluster from which an $E0$ transition to the ground state is forbidden. The 12.05-MeV level corresponds to 0^+ excitation of the core [$E_0 + (^{12}\text{C}) = 7.66$ MeV, $\rho(E0) = 0.72$] and single-quantum excitation of a cluster, and it must therefore have a large value of $\rho(E0)$. As can be seen from Table IV, such an interpretation is confirmed by the experimental data on monopole transitions.

The cluster structure of light nuclei is confirmed by microscopic Hartree–Fock calculations with an effective density-dependent interaction.[28] Such calculations, with allowance for deformation and projection onto states with definite spin, have shown that $4p4h$ configurations are energetically more advantageous than the $2p2h$ ones if they have an α-particle nature. At the same time, the minima of the total energy of the ^{16}O and ^{40}Ca nuclei for the ground states correspond to a spherically symmetric equilibrium shape of the nucleus but to a deformed shape for the excited 0_2^+ and 0_3^+ states.[29]

Details of the cluster structure can be studied experimentally in α-particle transfer reactions, for example, (^{6}Li, d). In recent years, great progress has been achieved here in not only the experimental investigation of the natural-parity states in sd- and pf-shell nuclei[30] but also in their theoretical description on the basis of the resonating-group method.[31]

Recently, light nuclei have been studied by the model of interacting bosons,[32] which takes into account phenomenologically the anharmonicity in the spectrum of elementary modes. In sd-shell nuclei ($16 < A < 40$) a restriction can be made to two-boson configurations: s^2 ($L = 0$), sd ($L = 2$), and d^2 ($L = 0, 2, 4$), by means of which the ground state

$$|0_1^+\rangle = \sqrt{1-\delta_0^2}\,|s^2(0)\rangle + \delta_0|d^2(0)\rangle \qquad (14')$$

and the first excited state

$$|2_1^+\rangle = \sqrt{1-\delta_2^2}\,|sd(2)\rangle + \delta_2|d^2(2)\rangle \qquad (14'')$$

are formed. Higher excitations are given by combinations orthogonal to (14). The mixing amplitudes $\delta_{0,2}$ are determined from the experimental energies and the quadrupole moment of the 2_1^+ level. As a result, this model reproduces the lower part of the spectrum in the Ne and Mg isotopes, in particular the observed change in the order in which the 0_2^+ and 2_2^+ levels follow on the transition from ^{20}Ne to ^{22}Ne, as is shown in Fig. 3.

LOW-LYING 0^+ STATES OF MAGIC NUCLEI

By virtue of their properties, magic nuclei and closed-shell nuclei occupy a distinguished position in nuclear physics. In the ground state, they have an "ideal" spherical shape. The spectra of excitations of magic nuclei are characterized by a lower level density and a higher energy of the first excited

TABLE IV. Cluster structure of 0^+ levels of the ^{16}O nucleus.

$E(0^+)$, MeV	Structure	$\rho(E0)/\rho_0(E0)$	
		Theory	Experiment
0	$\alpha + {}^{12}$C: $3s$	—	—
6,05	$\alpha + {}^{12}$C: $4s$	2	1,5 (2)
11,26	$\alpha + {}^{12}$C: $5s$	0	—
12,05	$\alpha + {}^{12}$C*: $4s$	2	1,7 (2)

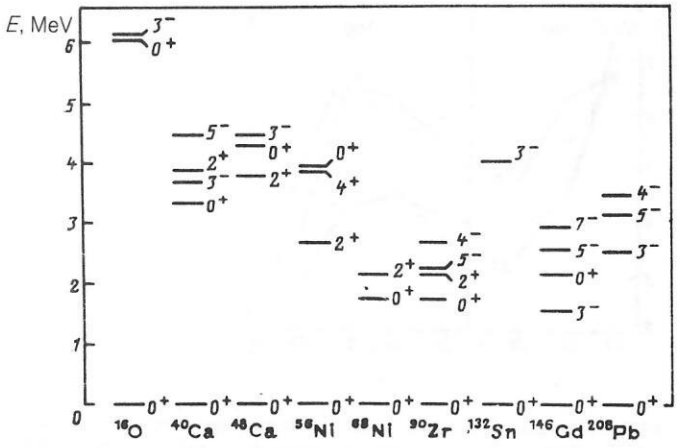

FIG. 4. Lowest levels of magic nuclei.[33,34]

state, which, as a rule, has spin–parity 3^- or 0^+ and not the usual 2^+ (Fig. 4).[33,34] In the region of high excitation energies of these nuclei giant multipole resonances, in particular a monopole resonance, are reliably allowed. The properties of odd nearly magic nuclei can be well described by the single-particle model. It is therefore natural to use it to analyze low-lying excitations in nuclei with closed shells or ones close to them in the framework of the particle–hole formalism. The unperturbed shell estimate for the energy of the lowest excited 0^+ state in magic nuclei appreciably exceeds the experimental values. An adequate description requires inclusion of many-particle correlations. The majority of calculations are made in the random-phase approximation using an effective interaction. The particular variants differ in the choice of the form of the interaction or the method of determining its parameters, in the single-particle model, and in the configuration space.[35] We must here mention the self-consistent calculations based on the Hartree–Fock method[28] or in the framework of the theory of finite Fermi systems.[36]

In the framework of the particle–hole formalism the description of low-lying states of positive parity in nuclei with closed shells involves some difficulties. First, it is necessary to know the nuclear single-particle spectrum in a wide range of energies. Second, since the excitation energy is about two intershell distances, $2p2h$ and more complicated configurations become important, and the part which they play is greater in light nuclei. For example, allowance for them in the ^{16}O nucleus lowers the calculated energy of the first 0^+ state from 13 to 9 MeV,[37] and satisfactory agreement with experiment is obtained only on $4p4h$ configurations.

Monopole properties of heavy nuclei such as the isotopic and isomer shifts, the $E0$ transitions between 0^+ states, and the energies of these states are to the greatest degree sensitive to the density dependence of the effective particle–hole interaction. It is therefore natural to choose its parameters with allowance for these data. Such calculations in the random-phase approximation led to excellent agreement between the theory and experiment for low-lying states with $I^\pi \neq 0^+$ in the ^{208}Pb nucleus.[38] However, for the energy of the first excited 0^+ state such calculations give a strongly overestimated value, the smallest of which is $E_{\text{theor}}(0_2^+) = 10.48$ MeV, whereas $E_{\text{exp}}(0_2^+) = 4.88$ MeV. This discrepancy cannot be eliminated by sensible variations of the interaction parameters. This indicates that the low-lying 0^+ states in magic nuclei are not coherent particle–hole superpositions of vibration type, in contrast to the 2^+, 3^-, etc., states.

Another approach assumes the occurrence of static deformation in the excited states, i.e., it is based on the idea of coexistence of different equilibrium shapes of the nuclear surface.[39] In the context of monopole excitations, a decisive argument is the fact that the first excited 0^+ states in the magic nuclei ^{16}O, ^{40}Ca, ^{90}Zr, which are spherical in the ground state, are the bases of rotational bands, i.e., they are deformed.

A static nuclear deformation arises as a result of a residual neutron–proton interaction between valence nucleons. In a closed-shell nucleus, the excitation of $2p2h$ configurations increases the number of valence nucleons and leads to the formation of deformed states. These are the so-called "intruder" analog states, which are most clearly manifested in transitional nuclei with one closed shell. The gain in the energy due to the quadrupole correlations and, therefore, the lowering of the 0^+ level are proportional to the number of nucleons (holes) of the other species outside the closed shells. This is illustrated in Fig. 5 by the systematic behavior of the energy of the intruder 0^+ states, whose properties cannot be explained by the vibration model, in Pb isotopes.[40] Qualitatively, the picture of intruder states is confirmed by microscopic calculations,[29,41] which give an additional minimum of the potential energy corresponding to a deformed 0^+ state for $2p2h$ and more complicated configurations.

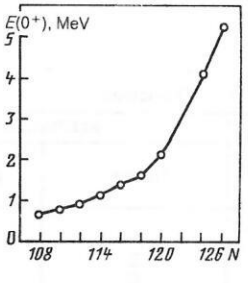

FIG. 5. Energies of intruder 0^+ levels in the $^{190\text{-}208}$Pb nuclei as functions of the number of neutrons.[40]

TABLE V. Energies of 0^+ levels and matrix elements of $E0$ transitions in magic nuclei.

Nucleus	$E(0_2^+)$, MeV	$\rho(E0;\ 0_2^+ - 0_1^+)$	$\rho_0(E0)$
^{40}Ca	3.353	0.17 (3)	0.20
^{48}Ca	4.272	0.10 (2)	0.19
^{90}Zr	1.752	0.058 (2)	0.16
^{146}Gd	2.162	0.10 (1)	0.13

Proton $2p2h$ configurations must be characterized by an $E0$-transition matrix element of order $\rho_0(E0)$. In heavy magic nuclei ($N>Z$) the density of neutron $2p2h$ configurations is higher. In conjunction with variations of the energy gap in the single-particle spectra, this may lead to a neutron $2p2h$ configuration making a large contribution to the wave function of the excited 0^+ states. This explains the decrease, compared with the estimate (8), of the observed $\rho(E0;\ 0_2^+ - 0_1^+)$ values in magic nuclei with increasing neutron excess, as shown in Table V.

The polarization effects due to addition of particles above closed shells reduce the rigidity of the nucleus with respect to monopole density oscillations. Besides lowering of the 0_2^+ level, this leads to large changes in the rms charge radii of the nuclei following excitation, as reflected in an increase in the matrix elements $\rho(E0;\ 0_2^+ - 0_1^+)$ compared with the magic nucleus. In Table VI, this is illustrated by the observed characteristics of the 0_2^+ states in Ca isotopes, in which the neutron $f_{7/2}$ shell is populated. In such cases, one speaks of effective neutron charges participating in the core polarization.

GIANT MONOPOLE RESONANCE

The experimental and theoretical investigation of giant resonances is a rapidly developing branch of nuclear physics. Many reviews (see, for example, Ref. 42) have described the situation in it. We here consider only specific questions associated with monopole resonances. An isoscalar monopole resonance corresponds to a so-called breathing mode, in which protons and neutrons move in phase. Isovector monopole resonances are polarization excitations in which the protons are displaced relative to the neutrons without a change in the total density. In the first mode, the restoring force is due to the nuclear compressibility; in the second, to the symmetry energy. The energy of isovector vibrations is always greater than that of isoscalar vibrations, since separation of the proton and neutron densities requires additional work.

The experimental energies of the isoscalar monopole resonances in even–even nuclei are shown in Fig. 6. To good accuracy, these energies can be described by the universal law

$$E\ (0^+) = (77 \pm 3)\, A^{-1/3}\ \text{MeV}. \tag{15}$$

The numerical coefficient was determined by means of all known centroid positions of $E0$ resonances irrespective of their method of excitation. Sample systematics of the energies of resonances excited, for example, in inelastic α-particle scattering gives the nearly equal value 75 MeV with a somewhat greater error.[43] The universal law (15) means that the energies of the monopole resonances are basically characterized by global characteristics of the nucleus and depend weakly on the details of its structure. This makes it possible to describe the breathing mode not only in macroscopic models but also in the framework of the microscopic approach.

It is well known that the liquid-drop model corresponds to the limiting case when the entire strength function is concentrated on one level. In this model[8,44] (with surface effects ignored), the energy of a monopole resonance is related to the compressibility K_∞ of nuclear matter (the compression modulus):

$$E\,(0^+) = \frac{\pi}{3}\,\frac{\hbar}{r_0}\sqrt{\frac{K_\infty}{m}}\,A^{-1/3}, \tag{16}$$

where m is the mass of a nucleon, and $r_0 = 1.2$ F is the radial parameter. With allowance for the parametrization (15), this leads to the value

$$K_\infty = (190 \pm 20)\ \text{MeV}. \tag{17}$$

The error in this value has a statistical nature and is due solely to the spread in the experimental data. The value (17) agrees well with the value $K_\infty \approx 200$ MeV determined from the isotopic shifts of x-ray lines.[45]

In accordance with the symmetry conditions, transitions of particles through two shells can contribute to the giant

TABLE VI. Energies of 0^+ levels and matrix elements of $E0$ transitions in Ca isotopes [$\rho_0(E0) \approx 0.20$].

Isotope	$E(0_2^+)$, MeV	$\rho(E0:\ 0_2^+ - 0_1^+)$
^{40}Ca	3.353	0.17 (3)
^{42}Ca	1.837	0.33 (5)
^{44}Ca	1.884	0.30 (2)
^{46}Ca	2.423	—
^{48}Ca	4.272	0.10 (2)

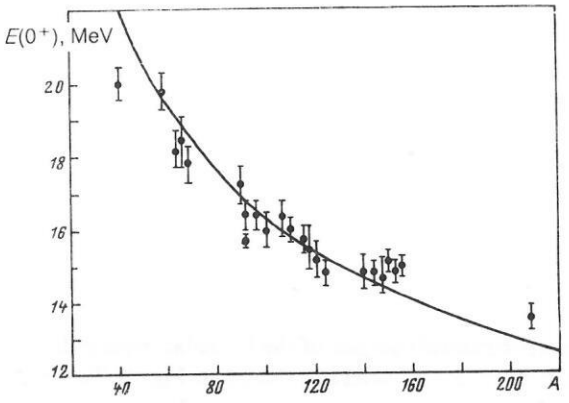

FIG. 6. Energies of isoscalar monopole resonances in even–even nuclei.

monopole resonance. The energy of such uncorrelated $1p1h$ configurations is about $2\hbar\omega_0 \approx 82A^{-1/3}$ MeV, a value that only slightly exceeds the observed values (15). Microscopic descriptions of $E0$ resonances have been obtained in models based on the Thomas–Fermi approximation, the cranking model, the time-dependent Hartree–Fock method, the method of K harmonics, the generator-coordinate method, and, finally, the random-phase approximation (see, for example, Ref. 46). In the harmonic limit of all these approaches Eq. (16) holds, so that in order to describe the energy of the monopole resonances it is sufficient to calculate the coefficient K_∞.

In self-consistent microscopic calculations based on the Hartree–Fock method, the giant resonances are described in the random-phase approximation by coherent superpositions of particle–hole configurations. A fundamental role is played here by the conditions of consistency between the average field and the effective interaction.[47] Violation of this connection leads to a sharp increase in the calculated energy or even to the destruction of the resonance. Calculations with realistic internucleon potentials give for K_∞ values between 100 and 200 MeV, and calculations with effective density-dependent forces give values greater than 190 MeV.[44,48]

The contribution of a giant monopole resonance to the energy-weighted sum rule (12) is determined by

$$s_1 = \int_{\Delta E} E\sigma(E)\,dE \Big/ \int_0^\infty E\sigma(E)\,dE, \tag{18}$$

where $\sigma(E)$ is the experimentally determined resonance cross section, and ΔE is the localization region of the resonance. Figure 7 gives the experimental values[43,49] of the ratio (18) and the results of theoretical calculations.[50] It can be seen that the main contribution of the resonance to the sum rule is well reproduced by the theory. The energy-weighted sum rules (10) can also be used to calculate the mean excitation energies

$$\overline{E}(0+) = \{m_1(E0)/m_{-1}(E0)\}^{1/2}, \tag{19}$$

which agree well with the experimental data.[46]

The experimentally observed widths of $E0$ resonances[43,49] are given in Fig. 8. They are appreciably greater

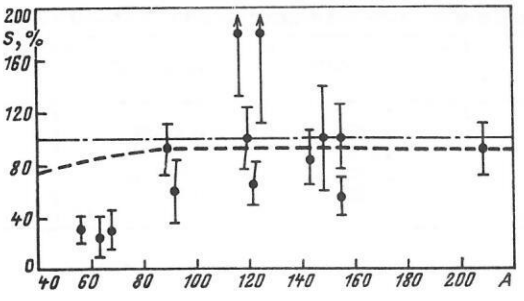

FIG. 7. Contribution of monopole resonances to the energy-weighted sum rule. The broken curve is the result of a microscopic calculation.[50]

than those calculated in the random-phase approximation taking into account only $1p1h$ configurations. This means that direct single-nucleon decay is not the main mechanism responsible for the width of the resonance. To describe the width and fine structure of the resonance, it is necessary to take into account as well more complicated configurations: $2p2h$ and those associated with low-lying phonons.[51–53] This greater complexity of the structure leads basically to a broadening of the localization region of the resonance, the position of its maximum remaining practically unchanged. This justifies the frequently employed resonance-broadening method, which is based on averaging the spectra calculated in the random-phase approximation over a certain energy interval.

VIBRATIONAL 0^+ STATES OF SPHERICAL NUCLEI

The shape of nuclei in the region $40 \lesssim A \lesssim 140$ or $190 \lesssim A \lesssim 220$, which have several particles or holes above closed shells, is spherically symmetric in the ground state. Their collective excitations correspond to vibrations of the nuclear surface about the equilibrium shape without change in volume. The dynamical variables in this case are the deformation parameters $\alpha_{\lambda\mu}$, which characterize the shape of the surface[8]:

$$R(\vartheta, \varphi) = R_0\left\{1 + \sum_{\lambda\mu} \alpha_{\lambda\mu} Y_{\lambda\mu}(\vartheta, \varphi)\right\}. \tag{20}$$

The monopole term ($\lambda = 0$) ensures conservation of the volume,

$$\alpha_{00} = -\frac{1}{\sqrt{4\pi}} \sum_{\lambda\mu} |\alpha_{\lambda\mu}|^2, \tag{21}$$

and the dipole term ($\lambda = 1$) corresponds to displacement of the nucleus as a whole and must be omitted.

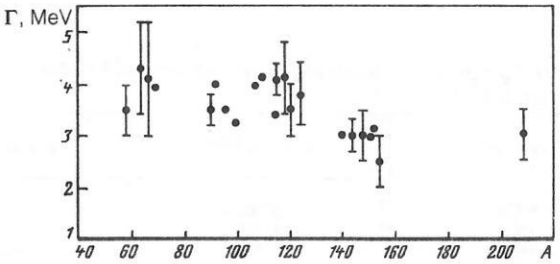

FIG. 8. Widths of giant monopole resonances.

The elementary excitations of surface vibrations can be regarded in the harmonic approximation as noninteracting quasiparticles—as phonons. Each phonon has spin λ and parity $(-1)^{\lambda}$. The excitation energy

$$E=\sum_{\lambda} n_{\lambda}\hbar\omega_{\lambda} \tag{22}$$

is determined by the number n_{λ} of phonons of each species. The frequencies

$$\omega_{\lambda}=\sqrt{C_{\lambda}/B_{\lambda}} \tag{23}$$

can be expressed in terms of the mass coefficients B_{λ} and the rigidity coefficients C_{λ}, which are regarded as parameters of the model.

In the hydrodynamical limit, these coefficients

$$B_{\lambda}^{\mathrm{hyd}}=3mAR_0^2/4\pi\lambda, \tag{24'}$$

$$C_{\lambda}^{\mathrm{hyd}}=(\lambda-1)(\lambda+2)R_0^2\sigma-\frac{\lambda-1}{2\lambda+1}\frac{3}{2\pi}\frac{e^2Z^2}{R_0} \tag{24''}$$

are determined solely by the multiplicity λ and the coefficient of surface tension σ, which can be taken from Weizsäcker's mass formula, $4\pi\sigma R_0^2\approx 20A^{2/3}$ MeV. These coefficients can be determined independently from the experimental values of the energy of the single-phonon level ($n_{\lambda}=1$) and the reduced probability of $E\lambda$ transition to the ground state:

$$B(E\lambda;\ n_{\lambda}=1\to n_{\lambda}=0)=\left(\frac{3}{4\pi}eZR_0^{\lambda}\right)^2\hbar/2\sqrt{B_{\lambda}C_{\lambda}}. \tag{25}$$

Such calculations for quadrupole excitations showed that the values of the parameters B_2 and C_2 differ strongly from the hydrodynamical values.[54]

In the majority of spherical nuclei, the experimental data confirm the vibrational nature of the low-lying excitations. The first excited 2^+ states correspond to quadrupole vibrations of the surface. The lowest 0^+ states in this model arise as two-phonon excitations of quadrupole type. Usually, octupole vibrations have an appreciably higher energy, and the corresponding 0^+ levels are not observed. An exception is the ^{208}Pb nucleus, in which the 0^+ state with energy 4.905 MeV has a two-phonon octupole nature.[55]

Figure 9 shows the ratios of the energies of the first excited 0^+ and 2^+ states of spherical nuclei. The deviation of these ratios from the vibrational limit could be due to several reasons. Small deviations can be explained by anharmonic effects associated with nonadiabaticity of the internal motion. In magic nuclei, in which $E(0_2^+)\approx E(2_1^+)$, the first 0^+ levels are not vibrational. Finally, growth of the ratio $E(0_2^+)/E(2_1^+)$ due to the denominator indicates a change in the equilibrium shape of the nucleus and the occurrence of static deformation. The first 2^+ state in these nuclei is associated with rotation and not vibrations of the surface.

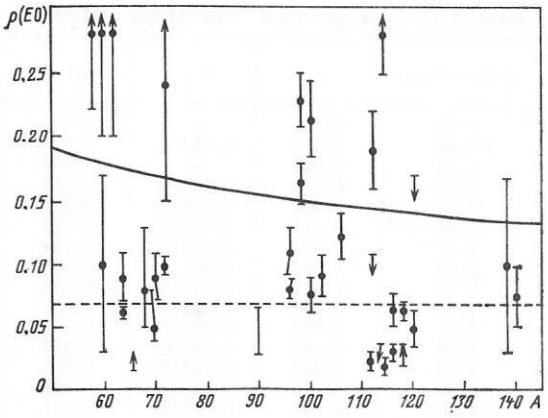

FIG. 10. Matrix elements of $E0$ transitions in spherical nuclei. The continuous curve is the single-particle estimate, and the broken line is the hydrodynamical estimate.

In terms of collective variables, the operator (4),

$$M(E0)=\frac{3}{4\pi}eZR_0^2\sum_{\mu}|\alpha_{2\mu}|^2, \tag{26}$$

is a two-quantum operator, and therefore the two-phonon 0^+ state must be coupled by a $E0$ transition to the ground state. The schematics of the observed monopole transitions from excited 0^+ states of spherical nuclei to the ground state is shown in Fig. 10.

The matrix element of $E0$ transition in the vibrational model,

$$\rho(E0;\ 0_2^+-0_1^+)=\sqrt{\frac{5}{2}}\frac{3}{4\pi}\frac{Z\hbar}{B_2\omega_2}=\sqrt{\frac{2}{5}}\frac{3}{4\pi}Z\beta^2, \tag{27}$$

is determined by the dynamical deformation parameter

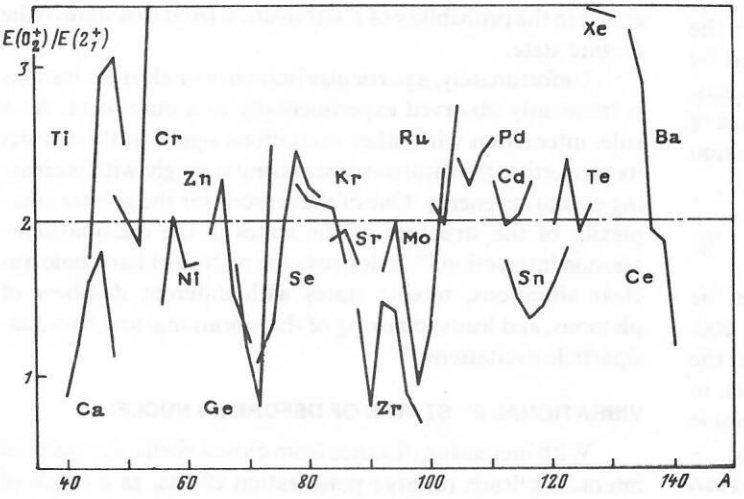

FIG. 9. Ratios of energies of the first excited 0^+ and 2^+ states in spherical nuclei.

TABLE VII. Characteristics of two-phonon 0^+ states of spherical nuclei.

Nucleus	$E(0_2^+) - E(2_1^+)$	β^2	X_{exp}	$\rho(E0)$	$\rho_{exp}(E0)$
^{40}Ca *	1.34	0.014	—	0.042	<0.06
^{42}Ca	1.21	0.059	0.043 (4)	0.178	0.33 (5)
^{44}Ca	1.63	0.048	—	0.145	0.30 (2)
^{60}Ni	1.72	0.045	0.027 (4)	0.188	0.03—0,17
^{66}Zn	2.28	0.051	0.047 (8)	0.232	>0.014
^{68}Zn	1.54	0.042	0.033 (2)	0.192	0.083 (40)
^{96}Mo	1.47	0.031	0.008 (2)	0.194	0.11 (2)
^{100}Ru	2.09	0.054	0.011 (1)	0.358	0.078
^{106}Pd	2.22	0.050	0.016 (3)	0.349	0.12 (2)
^{112}Cd	1.98	0.035	0.026 (1)	0.252	0.19 (3)
^{114}Cd	2.02	0.038	0.025 (1)	0.272	0.16 (1)
^{112}Sn	1.74	0.017	0.046 (8)	0.128	⩽0.11
^{114}Sn	1.50	0.014	0.042 (8)	0.106	0.16 (5)
^{116}Sn	1.36	0.013	0.023 (7)	0.096	0.066 (11)
^{118}Sn	1.43	0.013	0.009 (1)	0.101	0.072 (10)
^{120}Sn	1.60	0.013	0.007 (2)	0.095	0.051 (7)
^{122}Sn	1.83	0.014	0.046 (5)	0.106	—
^{206}Pb	1.46	0.001	—	0.017	0.031 (4)

*In the ^{40}Ca nucleus, the second excited 0^+ state with energy 5.213 MeV is considered.

$$\beta^2 = \left\langle \sum_{\mu} |\alpha_{2\mu}|^2 \right\rangle = \frac{5}{2} \hbar \Big/ \sqrt{B_2 C_2}\,. \tag{28}$$

The value of this parameter can be determined from the probability of $E2$ transition from the single-phonon 2_1^+ state to the ground state. The results of such calculations are given in Table VII, in which we give the values of the deformation parameter calculated in the framework of the vibrational model with data from the tables of Refs. 54 and 56. These values can be compared directly with the experimental ratio

$$X(E0/E2) = \frac{B(E0;\ 0_2^+ - 0_1^+);}{B(E2;\ 0_2^+ - 2_1^+)} = \beta^2, \tag{29}$$

which takes into account the features of the single-quantum $E2$ transition. Such an analysis of the decay properties of the low-lying 0^+ states of spherical nuclei indicates that their two-phonon nature corresponds to the experimental data. It is interesting that the hydrodynamical estimate (24) for the $E0$-transition matrix element gives a value practically independent of A, $\rho_{hyd}(E0) \approx 0.07$, for all spherical nuclei. In order of magnitude, this agrees with the experimental values (see Fig. 10).

The monopole moment is sensitive to the changes in the radial energy distribution. Equation (26) was derived by means of a homogeneous charge distribution in the nucleus. Allowance for a diffuse boundary leads to the appearance of an additional factor in the expression for the $E0$-transition operator:

$$\frac{3}{4\pi} eZR_0^2 \to \frac{3}{4\pi} eZR_0^2 \left[1 + \frac{\pi^2}{3}(2a_0/R_0)^2\right], \tag{30}$$

where a_0 is the diffuseness coefficient.[8] This increases the values of $\rho(E0)$ by about 30% at $A = 40$ and 10% at $A = 200$. As can be seen from Table VII, this correction improves the description of the $E0$ transitions in nearly magic nuclei, in which the polarization effects are small, and the harmonic approximation of the vibrational model must work well.

Single-phonon quadrupole states of spherical nuclei can be described microscopically by the "pairing-plus-quadrupole-forces" model.[10,57] The quadrupole-interaction parameter (MeV) determined from the consistency conditions,

$$\varkappa = 240\ (m\omega_0/\hbar)^2\ A^{-5/3}, \tag{31}$$

where $\hbar\omega_0 = 41A^{-1/3}$ MeV, agrees remarkably with the values calculated by RPA fitting of the energies of the first 2^+ levels for practically all spherical nuclei.

Besides the quadrupole two-phonon 0^+ states, there can also exist in spherical nuclei single-phonon states generated by various types of residual interaction, in the first place pairing[58,59] and spin–orbit[60] forces. The energy of the lowest 0^+ level of the pairing–vibrational branch lies in the region of the two-quasiparticle threshold. It is characterized by weak $E0$ and $E2$ transitions to the ground state and the first excited state. A specific test for this branch of nuclear excitations is provided by two-particle transfer reactions.[61] The introduction of spin–orbit forces leads to the appearance of a below-gap 0^+ level with a high degree of collectivization and strongly interfering with the pairing vibrations.[62] The monopole nature of the spin–orbit forces is manifested in an increase in the probability of $E0$ transition from this state to the ground state.

Unfortunately, a particular branch of nuclear excitations is frequently observed experimentally in a pure form. As a rule, interaction with other excitations significantly distorts its properties, the distortion increasing strongly with increasing excitation energy. One of the reasons for the greater complexity of the structure of the states is the quasiparticle–phonon interaction.[63] It destroys the picture of harmonic nuclear vibrations, mixing states with different numbers of phonons, and leads to mixing of the vibrational and two-quasiparticle excitations.[64]

VIBRATIONAL 0^+ STATES OF DEFORMED NUCLEI

With increasing distance from closed shells, the residual interaction leads to large polarization effects, as a result of

which the nucleus acquires a static deformation. Three regions of deformed nuclei are well known: the region of light nuclei of the *sd* shell, $20 \leqslant A \leqslant 30$, the region of rare-earth nuclei, $150 \lesssim A \lesssim 190$, and the transuranium region, $A \gtrsim 220$.

The various models that treat the properties of low-lying excitations of deformed nuclei are based on the rotational–vibrational Hamiltonian[8,65]

$$H = \sum_{k=1}^{3} \frac{I_k^2}{2J_k(\beta, \gamma)} - \frac{\hbar^2}{2B}\left\{\frac{1}{\beta^4}\frac{\partial}{\partial\beta}\beta^4\frac{\partial}{\partial\beta} + \frac{1}{\beta^2\sin 3\gamma}\frac{\partial}{\partial\gamma}\sin 3\gamma\frac{\partial}{\partial\gamma}\right\} + V(\beta, \gamma). \quad (32)$$

The first term here is the energy of rotation with moments of inertia dependent on the shape parameters β and γ, which determine the total deformation and the departure of the nuclear shape from axial symmetry. The second term is the kinetic energy of the vibrations of the nuclear surface, characterized by the mass coefficient B. In the general case, the energy $V(\beta,\gamma)$ can be a function of the two invariants β^2 and $\beta^3\cos 3\gamma$ with respect to three-dimensional rotations.[66] The actual models differ in the choice of this functional dependence. Frequently, the choice is dictated by considerations of simplicity and convenience. The physical significance of the introduction of the new coordinates is in the possibility of independent treatment of rotation of the deformed nucleus as a whole and of the vibrations associated with the change in its shape.

For small quadrupole harmonic vibrations about the axisymmetric equilibrium shape characterized by a deformation parameter β_0, the potential energy is

$$V(\beta, \gamma) \approx \frac{1}{2}C_\beta(\beta-\beta_0)^2 + \frac{1}{2}C_\gamma\beta_0^2\gamma^2. \quad (33)$$

In this case, two types of vibrations of the nuclear surface are possible: β vibrations, which deform the ellipsoid along the symmetry axis and preserve the axial symmetry, and γ vibrations, which correspond to vibrations in the perpendicular plane for which the axial symmetry is broken. To these vibrations there correspond states with K^π equal to 0^+ and 2^+, these being the bases of β- and γ-vibrational bands in the deformed nuclei.

In the adiabatic approximation, when there is no coupling between rotation and the vibrations, the energies of the low-lying excited states of the deformed nuclei,[9]

$$E = \frac{\hbar^2}{2J}\{I(I+1) - K^2\} + n_\beta\hbar\omega_\beta + \left(2n_\gamma + \frac{K}{2}\right)\hbar\omega_\gamma, \quad (34)$$

are determined solely by the spin I, its projection K, and the numbers $\eta_{\beta,\gamma}$ of vibrational quanta of each type. The effective moment of inertia J and the frequencies $\omega_{\beta,\gamma} = \sqrt{C_{\beta,\gamma}/B}$ are parameters of the model. In principle, they can be calculated microscopically,[67] but they are usually determined from the experimental energies and probabilities of $E2$ transitions.[9] For rigid nuclei, for which the vibration amplitudes are small, i.e., $|\beta-\beta_0| \ll \beta_0$ and $\gamma \ll 1$, the operator (26),

$$M(E0) = \frac{3}{4\pi}eZR_0^2\beta^2 \approx 2\frac{3}{4\pi}eZR_0^2\beta_0(\beta-\beta_0), \quad (35)$$

gives for the matrix element of the $E0$ transition from states of the β band to the ground-state band the expression

$$\rho(E0;\ I,\ n_\beta = 1 \to I,\ n_\beta = 0) = \frac{3\sqrt{2}}{4\pi}Z\beta_0\sqrt{\hbar/B\omega_\beta}, \quad (36)$$

which does not depend on the spin. As can be seen from Table VIII, the experimental values of $\rho(E0)$ do indeed depend weakly on the spin of the states, i.e., the condition of adiabaticity for the $E0$ transitions in these nuclei is well satisfied. However, the values of the parameters in (36) calculated from the energies of the 0^+ levels and the $E2$-transition probabilities (the quadrupole moments) lead to values of the matrix element $\rho(E0)$ that are too large.

The parameter of the mixing of the $E0$ and $E2$ transitions from the β band to the ground-state band has in the adiabatic limit a simple spin dependence ($I \geqslant 2$):

$$X_I(E0/E2) = \frac{B(E0;\ I \to I)}{B(E2;\ I \to I)} = X_0(E0/E2)\frac{(2I-1)(2I+3)}{I(I+1)}, \quad (37)$$

where

$$X_0(E0/E2) = \frac{B(E0;\ 0_2^+ - 0_1^+)}{B(E2;\ 0_\beta^+ - 2_1^+)} = 4\beta_0^2 \quad (38)$$

depends only on the equilibrium-deformation parameter. As is shown in Table IX, the ratios X_I/X_0 calculated from the experimental data agree to within the errors with the theoretical values. The parameter $X_0(E0/E2)$ can be determined independently from the quadrupole moments of the nuclei.[68] The results of such a calculation appreciably exceed the experimental values (Fig. 11). This discrepancy can be due to nonadiabaticity of the collective motion in the nucleus as well as to the fact that the first excited 0^+ state has a nature more complicated than that of simple β vibrations. Allowance for coupling of the rotational and vibrational modes, for example, reduces the theoretical value of $X_0(E0/E2)$ by about two times.[69] The same effect leads to a difference between the

TABLE VIII. Matrix elements of $E0$ transitions between states of the β band and the ground-state rotational band.

I	^{152}Sm	^{154}Gd	^{156}Gd	^{174}Hf
0	0.23 (3)	0.30 (1)	0.20 (3)	0.220 (25)
2	0.25 (2)	0.29 (2)	0.23 (5)	0.23 (2)
4	0.24 (5)	0.19 (6)	0.22 (3)	0.20 (3)
6	—	0.25 (2)	—	0.22 (3)
8	0.21 (6)	$\geqslant$0.20	—	—
10	0.28 (10)	—	—	—

TABLE IX. Spin dependence of the ratio X_I/X_0 ($E0/E2$) for transitions from the β band to the ground-state band.

I	Adiabatic limit	^{152}Sm	^{152}Gd	^{154}Gd	^{156}Gd	^{156}Dy	^{164}Er
2	3.50	3.9 (9)	5.0 (18)	4.8 (13)	1.9—5.2	>2.5	2.1 (7)
4	3.85	6.0 (30)	4.9 (10)	5.0 (22)	2.0—6.9	>3.3	7.2 (45)
6	3.93	—	—	3.8 (17)	>2	>2.7	—
8	3.96	—	—	5.3 (28)	—	>3.5	—
10	3.97	—	—	3.0 (23)	—	—	—

moments of inertia corresponding to the rotational bands based on the ground state and the β-vibrational state of the deformed nuclei. Figure 12 shows the ratios of the moments of inertia J_β/J_0 calculated from the excitation energies of the corresponding 2^+ states.[70] The blocking effect decreases the pairing correlations in excited states and, therefore, increases the moment of inertia.[10] Decrease in the moment of inertia J_β may be due to decrease in the deformation parameter in the excited state. Indeed, in nuclei for which $J_\beta/J_0 < 1$ the deformation parameter in the β-vibrational 0^+ state calculated by means of (38) from the observed $X_0(E0/E2)$ values is less than the equilibrium value.

The theory of nuclei that are nonaxial in the ground state has been presented in detail in Ref. 65. In this approach, excited states with $K^\pi = 2^+$ form an anomalous rotational band and are associated, not with γ vibrations, but with rotation of the nonaxial nucleus around the major axis of the ellipsoid. The energy of the first 0^+ level from the band of γ vibrations with $K^\pi = 0^+$ (this energy is determined by the rigidity parameter C_γ) can be estimated from the simple relation

$$E(0_\gamma^+) = 2E(2_a^+) - E(2_1^+), \tag{39}$$

where $E(2_a^+)$ is the energy of the first 2^+ level of the anomalous band. At the present time, 0^+ states can be identified in several deformed nuclei, as is done in Table X. These states are well localized with respect to the energy, i.e., the distance between the predicted 0_γ^+ level and the nearest 0^+ state in the spectrum of the nucleus is much less than the energy intervals between the monopole states. We note that in the ^{166}Er, ^{188}Os, and ^{190}Pt nuclei the 0_γ^+ state is the first excited 0^+ state.

In the model of a nonaxial rotator an expression equivalent to (36) is valid for $E0$ transitions between states of the β-vibrational band and the ground-state rotational band. The ratio $X(E0/E2)$ is somewhat larger than (38), namely,

$$X_\beta = 4\beta_0^2(1 + 1/s), \tag{40}$$

where $s = E(2_a^+)/E(2_1^+)$. The matrix element of $E0$ transition from levels of the γ-vibrational band to the ground-state band,

$$\rho(E0;\ I,\ n_\gamma = 1 \to I,\ n_\gamma = 0) \approx 0.65Z\beta_0^3/(2s-1), \tag{41}$$

is appreciably less than (36), in agreement with the existing experimental data. The ratio

$$X_\gamma = \frac{B(E0;\ 0_\gamma^+ - 0_1^+)}{B(E2;\ 0_\gamma^+ - 2_1^+)} \approx 36\beta_0^2(1 - q^2/s^2)^{-2}, \tag{42}$$

where $q = E(0_\beta^+)/E(2_1^+)$, can take very large values for the 0_γ^+ state in nuclei in which the energies of the 0_β^+ and 2_a^+ states are comparable. Figure 13 shows the ratio of (42) and (40), which does not depend on the deformation β_0, as a function of the parameter $E(0_\beta^+)/E(2_a^+)$. The points corresponding to the experimental values of the quantities that occur here lie remarkably well on the theoretical curve. This is a

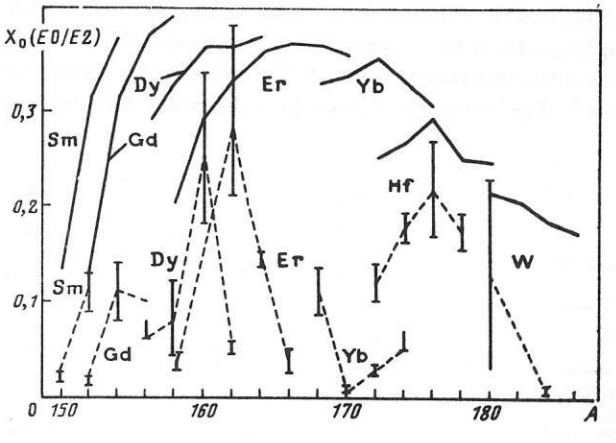

FIG. 11. The ratio $X_0(E0/E2)$ for the first excited 0^+ states of deformed nuclei. The continuous lines connect the theoretical values, and the broken lines connect the experimental points.

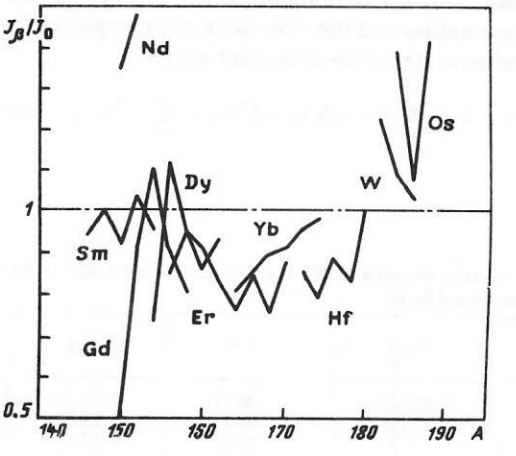

FIG. 12. Ratios of effective moments of inertia for the β band and the ground-state rotational band of deformed nuclei.

TABLE X. Energies of 2^+ levels of the ground-state and anomalous rotational bands, 0^+_γ states, and 0^+ levels closest to them in the spectrum of deformed nuclei, MeV.

Nucleus	$E(2^+_1)$	$E(2^+_a)$	$E(0^+_\gamma)$	$E_{exp}(0^+)$
^{146}Sm	0.747	1.648	2.549	0^+_4: 2.611
^{148}Sm	0.550	1.454	2.358	0^+_3: 2.358
^{158}Dy	0.099	0.946	1.793	0^+_3: 1.665
^{160}Dy	0.087	0.966	1.845	0^+_4: 1.953
^{162}Dy	0.081	0.888	1.695	0^+_4: 1.670
^{158}Er	0.192	0.820	1.448	0^+_3: 1.387
^{164}Er	0.091	0.860	1.629	0^+_4: 1.702
^{166}Er	0.081	0.786	1.491	0^+_3: 1.460
^{168}Yb	0.088	0.984	1.880	0^+_4: 1.904
^{182}W	0.100	1.221	2.342	0^+_4: 2.284
^{184}W	0.111	0.903	1.695	0^+_4: 1.615
^{186}Os	0.137	0.768	1.399	0^+_3: 1.456
^{188}Os	0.155	0.633	1.111	0^+_2: 1.086
^{190}Pt	0.296	0.598	0.900	0^+_2: 0.922

strong argument for a single-phonon nature of the γ-vibrational 0^+ states of deformed nuclei.

The two variants of the rotational–vibrational model have the same number of parameters, determined by the same experimental data. The main difference arises in the treatment of $E0$ transitions from states of the anomalous band ($K^\pi = 2^+$) to the ground-state band. In the adiabatic approximation, they are forbidden with respect to K and take place only by virtue of band mixing. Therefore, the observed values of $\rho(E0)$ and $X(E0/E2)$ for transitions from the anomalous 2_a^+ level to the 2^+ level of the ground-state rotational band in rigid nuclei are less than the analogous values for 2^+ states from the β band by an order of magnitude and more.[71] For a nucleus that is axisymmetric in the ground state

$$\rho(E0;\ 2_a^+ - 2_1^+) \approx 1.35 Z\beta_0^2/\sqrt{2s-1}\,[q^2-(s-1)^2], \quad (43)$$

and for a nucleus that is nonaxial but sufficiently rigid with respect to γ vibrations

$$\rho(E0;\ 2_a^+ - 2_1^+) \approx 5.16 Z\beta_0^3\Gamma^4 \sin 3\gamma_0/\sqrt{9-8\sin^2 3\gamma_0}, \quad (44)$$

where $\Gamma^{-2} \approx 2s-1$ ($\Gamma < 0.3$), and γ_0 is the parameter of the equilibrium nonaxiality.[65] Results of different calculations of $\rho(E0)$ and $X(E0/E2)$ for these transitions were compared in Ref. 4. Figure 14 shows some of these results together with the available experimental data.

The observation of two-phonon states in deformed nuclei is more difficult than in spherical nuclei, since for such nuclei they belong to a region of energies in which there are not only large numbers of rotational levels but also many two-quasiparticle and single-phonon states. In the quasiparticle–phonon nuclear model[73] it has been concluded that there are no two-phonon states in deformed nuclei, a result that is confirmed by analysis of the experimental data.[74] In particular, for the 0^+ levels with energies 1.217, 1.422, and 1.834 MeV the admixture of two-phonon components is less than 5%. This agrees with experimental data on (p,t) and (t,p) reactions. In the spectra of the heavy Ra, Th, and U nuclei there are no two-phonon 0^+ states of octupole type with energy in the region of twice the energy of the state with $I^\pi K = 1^-0$.

Numerous studies have been devoted to microscopic investigation of single-phonon 0^+ states of deformed nuclei (see, for example, Ref. 3). In the "pairing-plus-quadrupole-forces" model,[10] it is possible to achieve only a qualitative description, this indicating that the nature of the first excited

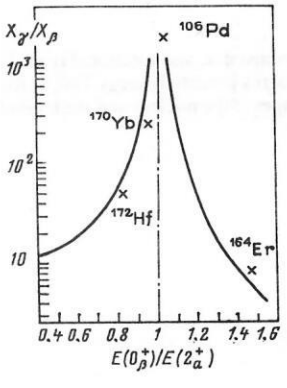

FIG. 13. The ratio X_γ/X_β as a function of the parameter $E(0^+_\beta)/E(2^+_a)$. The crosses are the experimental points.

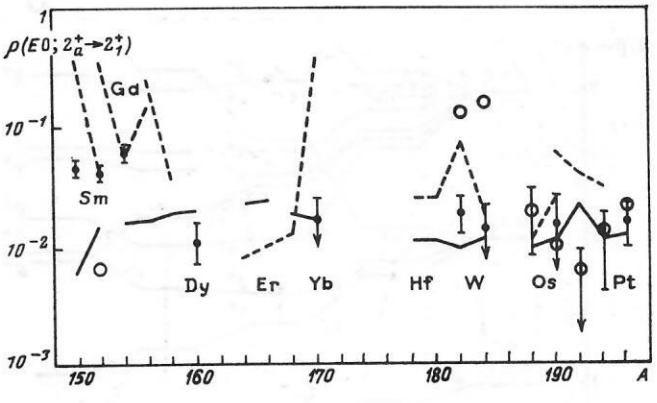

FIG. 14. Matrix elements of $E0$ transitions from 2^+ states of the anomalous rotational band to the ground-state band. The continuous lines connect the results of calculations in the model of a nonaxial rotator[65]; the broken lines, the results obtained in the rotational–vibrational model.[71] The open circles are the results of a microscopic calculation.[72]

0^+ states is more complicated than that of the 2^+ states. Numerical calculations in a model with a separable interaction consistent with the average-field potential[75] showed that to achieve agreement between theory and experiment it is not sufficient to take into account only the particle–hole interaction; pairing must also be taken into account in a self-consistent manner.

To describe several 0^+ levels observed experimentally below the two-quasiparticle threshold, additional types of interaction have been introduced into the theory: monopole,[76] hexadecapole,[77] spin-quadrupole,[78] spin–orbit[79] in the particle–hole channel, and multiple pairing in the particle–particle channel.[80] The best results were apparently obtained in Ref. 81, which used a density-dependent effective particle–hole interaction and a δ-function interaction in the particle–particle channel.

MONOPOLE STATES OF TRANSITIONAL NUCLEI

Nuclei whose spectra occupy an intermediate position between vibrational and rotational spectra are usually classified as transitional. In the study of the properties of these nuclei, the effects of the zero-point vibrations of the average field, which are not taken into account in the collective Hamiltonian (32), are particularly important. Figure 15 shows the transition from the vibrational to the rotational type of nuclear spectrum in its dependence on the depth of the minima of the potential energy $V(\beta,\gamma)$ corresponding to prolate and oblate shape and on the position of the level of the zero-point vibrations.[82] It can be seen that the deviation from the vibrational type is due to the softness of the potential with respect to the nonaxiality parameter.

In the intermediate situation of an anharmonic γ-soft vibrator, the first excited 0^+ state is by nature a three-phonon state. The 0^+ level with energy 1.760 MeV in the ^{134}Ba nucleus can serve as an example of this. For it, the experimentally measured ratio of the single-quantum $E2$ transition to the 2_2^+ state to the two-quantum transition is $B(E2;0_2^+-2_2^+)/B(E2;0_2^+-2_1^+)=28$.[83] The large observed value of the ratio $X(E0/E2)\approx 2.9$ confirms this interpretation. For the following 0^+ levels in this nucleus, $X(E0/E2)\lesssim 10^{-2}$.

In even–even nuclei with $N\simeq 40$ or $Z\simeq 40$, the experimental data indicate an abrupt lowering of the excitation energy of the 0_2^+ level (see Fig. 9). In the ^{72}Ge, ^{96}Zr, and ^{98}Mo nuclei it is the first excited state, as in the magic nuclei ^{68}Ni and ^{90}Zr. To explain this anomaly at the microscopic level, shell calculations have been used,[84] but a model with mixing of a two-phonon (four-quasiparticle) 0^+ state with pairing vibrations proved to be the most fruitful. In a large group of nuclei, from ^{66}Zn to ^{122}Sn, good agreement with experiment for the energies of the monopole states and the values of $B(E2;0_2^+-2_1^+)$ and $\rho(E0;0_2^+-0_1^+)$ was obtained.[85] In Fig. 16, the results of calculations of the energies $E(2_1^+)$ and $E(0_n^+)$ for Ge isotopes are compared with experimental data.[86] An admixture of a monopole phonon of pairing vibrations in the wave function is needed to reproduce the observed probabilities of the electromagnetic transitions and the amplitudes of two-particle transfers. The calculated shape of the surface of these nuclei is transitional from prolate to oblate, in agreement with the ideas of the collective model.

Phenomenologically, details in the spectra of transitional nuclei exhibiting both vibrational and rotational properties can be described by a model with intruder analog states corresponding to different equilibrium deformations. In nuclei having few valence nucleons of one type (near the magic numbers 40 or 50), their number can increase because of transitions through a shell. Energetically, this is compensated by the residual interaction. In the simplest case, such $2p2h$ con-

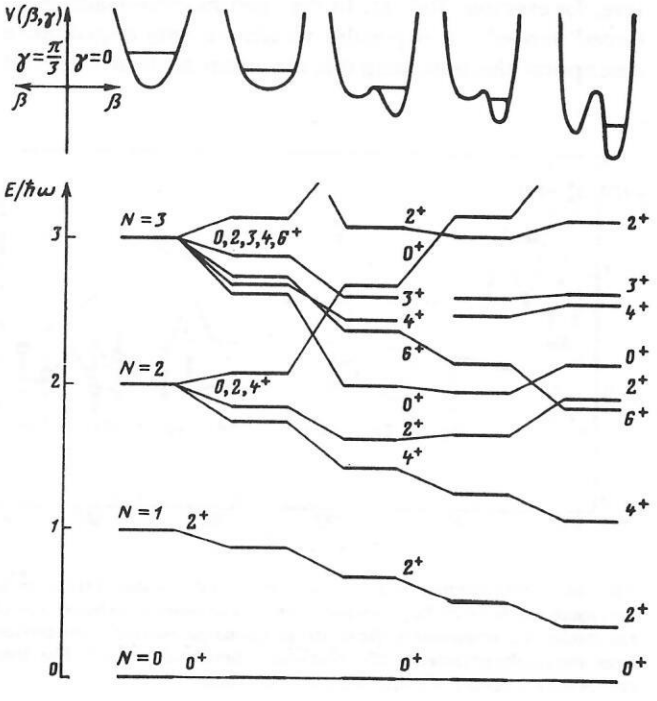

FIG. 15. Nuclear spectra of vibrational, γ-unstable, and rotational types.[82] At the top of the figure we show the form of the potential energy $V(\beta,\gamma)$ for prolate ($\gamma=0$) and oblate ($\gamma=\pi/3$) shapes of the nucleus and the level of the zero-point vibrations.

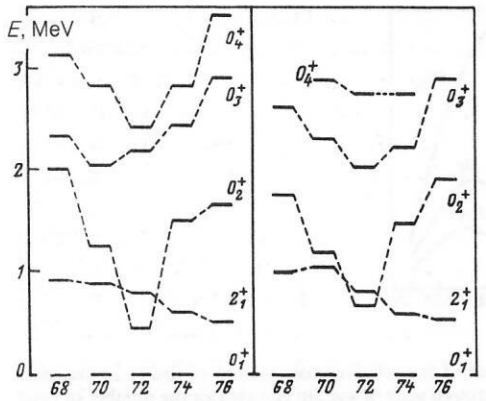

FIG. 16. Energies of the first 2^+ levels and 0^+ levels in the Ge isotopes.[86] The results of calculations are given on the left, and the experimental data on the right.

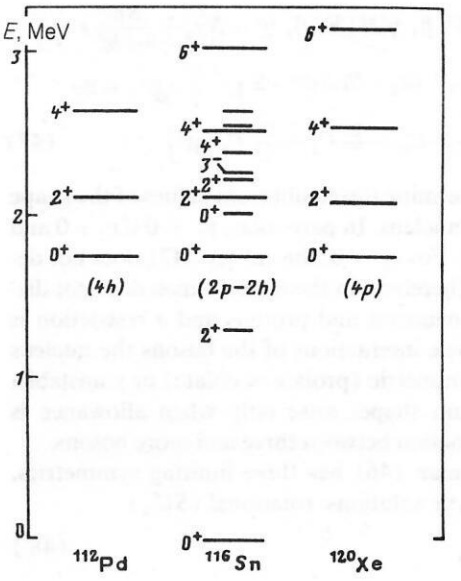

FIG. 17. Ground-state rotational bands in ^{112}Pd and ^{120}Xe and intruder analog states in ^{116}Sn.[90] The energies of the ground states of the deformed nuclei are reduced to the energy of the first excited 0^+ state in ^{116}Sn; the vibrational levels are identified by the shorter lines.

figurations make it possible to speak of the coexistence of shapes in nuclei of the *fpg* shell.[87] At the same time, as occurs in magic nuclei, the ground state usually has an almost spherical shape, while the first excited 0_2^+ state is deformed and is the base of a rotational band. In the ^{74,76}Kr nuclei, the situation is the opposite, i.e., the ground state is deformed.[88]

The idea of coexistence of shapes received strong experimental support in the even isotopes of tin. In them, the first 0^+ states are strongly excited in (^{3}He,n) reactions, and this permits interpretation of them as proton $2p2h$ configurations. These states are the bases of rotational bands excited in (α,$2n$) reactions. Detailed spectroscopic investigation of these isotopes reveals a complicated mixture of proton $2p2h$ configurations with quadrupole vibrations of a spherical core.[89]

If the idea of intruder states is correct, then in this nucleus one must observe a class of $2p2h$ excitations containing the same correlations as the ground-state bands of the neighboring nuclei having four particles or holes above a closed shell. For example, in the ^{116}Sn nucleus with 16 valence neutrons one must observe proton $2p2h$ excitations having a structure (energies, transition probabilities, etc.) similar to the ground-state bands in ^{112}Pd and ^{120}Xe. Figure 17 shows the spectra of these nuclei. It can be clearly seen that after separation of the intruder analog states there remain levels of only vibrational type. This evidently explains the employed terminology. A similar systematics is obtained for the ^{110}Ru, ^{114}Cd, ^{118}Te, and ^{122}Ba nuclei.[90]

Analysis of cross sections of the (^{6}Li, d) and (d, ^{6}Li) reactions taking place to the ground and the first excited 0^+ state of Ge isotopes showed that in the wave function of the intruder 0_2^+ state of the ^{72}Ge nucleus there is a large component corresponding to α-particle excitation.[91] The short-range attractive correlations in this state give an additional gain in the energy and explain the lowering of the corresponding level. The amplitude of the admixture of the α-particle component, determined independently from cross sections of the α- and $2n$-transfer reactions, agrees well with the observed value of the matrix element of $E0$ transition to the ground state.

Recently, the interacting-boson model (see, for example, Refs. 92 and 93) has been widely used to describe the properties of transitional nuclei. In this model, the positive-parity levels are regarded as excitations in a gas of interacting bosons. Phenomenologically, it is possible to make a restriction to just monopole (s) and quadrupole (d) collective bosons, in accordance with the symmetry of the lowest excited states and with allowance for the decisive part played by the quadrupole surface vibrations and monopole pairing vibrations.

The normalized boson state for $2N$ valence electrons (in the simplest version of the model, no distinction is made between neutrons and protons),

$$|N;\ \beta,\ \gamma\rangle = [N!\,(1+\beta^2)^N]^{-1/2}\,(B^+)^N|0\rangle, \qquad (45')$$

where

$$B^+ = s^+ + \beta\left\{\cos\gamma\, d_0^+ + \frac{1}{\sqrt{2}}\sin\gamma\,(d_2^+ + d_{-2}^+)\right\}, \qquad (45'')$$

is equivalent to the intrinsic state of the rotational–vibrational model.[94] The advantage is associated with felicitous parametrization, which makes it possible to separate the γ-unstable limit.

The most general form of Hamiltonian with pairing boson interactions,

$$H = \varepsilon_s s^+ s + \varepsilon_d d^+\tilde{d} + u_0 s^+ s^+ ss + u_2 s^+ d^+\,\tilde{d}s + v_0\,(d^+ d^+ ss + s^+ s^+ \tilde{d}\tilde{d}) + v_2\,\{[d^+ d^+]_2\,\tilde{d}s + s^+ d^+\,[\tilde{d}\tilde{d}]_2\} + \sum_L C_L\,[d^+ d^+]_L\,[\tilde{d}\tilde{d}]_L, \qquad (46)$$

where $\tilde{d}_\mu = (-1)^\mu d_{-\mu}$ and ε_s, $\varepsilon = \varepsilon_d - \varepsilon_s$, $u_{0,2}$, $v_{0,2}$, and $C_{0,2,4}$ are parameters of the model, leads to the simple energy surface

$$E_N(\beta, \gamma) = \langle N; \beta, \gamma | H | N; \beta, \gamma \rangle = N\varepsilon_s + \frac{N\beta^2}{1+\beta^2}\varepsilon + \frac{N(N-1)}{(1+\beta^2)^2}\left\{u_0 + (u_2 + 2v_0)\beta^2 - 2\sqrt{\frac{2}{7}}v_2\beta^3\cos 3\gamma + \left(\frac{1}{5}C_0 + \frac{2}{7}C_2 + \frac{18}{35}C_4\right)\beta^4\right\}, \quad (47)$$

whose minima determine the equilibrium values of the shape parameters of the nucleus. In particular, $\gamma_0 = 0$ if $v_2 > 0$ and $\gamma_0 = \pi/3$ if $v_2 < 0$. For $v_2 = 0$, the energy (47) does not depend on γ at all. Therefore, in the model which does not distinguish between neutrons and protons and a restriction is made to two-particle interactions of the bosons the nucleus can be either axisymmetric (prolate or oblate) or γ unstable. Triaxial equilibrium shapes arise only when allowance is made for the interaction between three and more bosons.

The Hamiltonian (46) has three limiting symmetries, which admit analytic solutions: rotational (SU_3)

$$H_3 = \varkappa_3 Q_3 Q_3, \quad (48')$$

for $u_0 = 0$ and $\varkappa_3 = (1/5)$ $\varepsilon_s = (4/11)$ $\varepsilon_d = (1/2)$ $u_2 = v_0 = -(1/\sqrt{7})$ $v_2 = (4/7)$ $C_0 = -(8/3)$ $C_2 = 2C_4$ (the case $\varkappa_3 < 0$; is physically interesting); vibrational (SU_5)

$$H_5 = \varepsilon_d d^+\tilde{d} + \varkappa_5 d^+ d^+ \tilde{d}\tilde{d}, \quad (48'')$$

if only ε_d and $C_0 = 5\varkappa_5$ are nonzero; γ-unstable (O_6)

$$H_6 = \varkappa_6 Q_6 Q_6 \quad (48''')$$

for nonvanishing coefficients $\varkappa_6 = (1/5)$ $\varepsilon_s = \varepsilon_d = (1/2)$ $u_2 = v_0$ ($\varkappa_6 < 0$). The type of a nucleus in the transitional region between these symmetries is determined by the ratio of the characteristic parameters in the Hamiltonian (46). For example, magic nuclei correspond to the region between the SU_5 and O_6 limits. Proximity to the γ-unstable limit made it possible to find an easy explanation for the observed predominance of the decay of all excited 0^+ states to the 2_2^+ level in the Os isotopes as compared with the mixed decay to the 2_1^+ and 2_2^+ levels in the Pt isotopes.[92]

The operators of the electromagnetic transitions in the interacting-boson model are constructed in accordance with the general rule for single-particle tensor operators. In particular,

$$M(E0) = \frac{1}{\sqrt{5}}\beta_0 d^+\tilde{d} + \gamma_0 s^+ s. \quad (49)$$

In Table XI, calculations[95] of the matrix elements $\rho(E0)$ are compared with experimental data for the ^{114}Cd nucleus.

In the limiting cases (48) of the model there exist analytic expressions for the amplitudes of two-particle transfers between the ground states of the nuclei[92]:

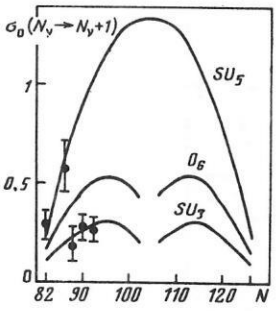

FIG. 18. Dependence of the relative cross section of the (t, p) reaction taking place to the ground state of the Sm isotopes on the number of neutrons.[92]

$$S_0(N \to N+1) = \begin{cases} \alpha^2 \frac{(N+1)(2N+3)}{3(2N+1)}\left\{\Omega - N - \frac{4N(N-1)}{3(2N-1)}\right\}, & SU_3, \\ \alpha^2 (N+1)\left(\frac{\Omega}{2} - N\right), & SU_5, \\ \alpha^2 \frac{(N+1)(N+4)}{2(N+2)}\left\{\Omega - N - \frac{N(N-1)}{2(N+1)}\right\}, & O_6, \end{cases} \quad (50)$$

where α^2 is a normalization factor which reflects the coherence of the fermion pairs, and Ω is the maximal number of nucleons in a shell. The first two expressions of (50) describe well the observed cross sections of (t, p) reactions on the Sm isotopes, and the third describes those on the Os and Pt isotopes, as is shown in Figs. 18 and 19. Besides the dependence on the number N of bosons, the expressions (50) show that in the limit of large N the amplitudes S_0 for the SU_5 and SU_3 symmetries differ appreciably. The experimental data given in Fig. 18 illustrate the transition from one symmetry to another with increasing number of neutrons. The data on the (t, p) reactions taking place to the ground state of the Os and Pt isotopes (Fig. 19) match unambiguously the O_6 limit. This confirms the γ instability of these nuclei deduced from analysis of their spectra.

The effective boson Hamiltonian can be constructed microscopically by the method of boson expansions of the fermion operators.[93,96] The interacting-boson model corresponds to truncation of the resulting series, the coefficients of which are regarded as adjustable parameters. The literal interpretation is tantamount to neglect in this model of the interaction in the particle–hole channel, for which no physical grounds are evident.[97]

TABLE XI. $E0$ transitions in ^{114}Cd in the interacting-boson model.[95]

$I_i^\pi - I_f^\pi$	$\rho_{\text{theor}}(E0)$	$\rho_{\text{exp}}(E0)$
$0_2^+ - 0_1^+$	0.277	0.164
$0_3^+ - 0_1^+$	0.068	0.039
$0_3^+ - 0_2^+$	0.033	0.020
$2_2^+ - 2_1^+$	0.045	<0.09
$2_3^+ - 2_1^+$	0.16	0.25
$2_3^+ - 2_2^+$	0.05	0.18

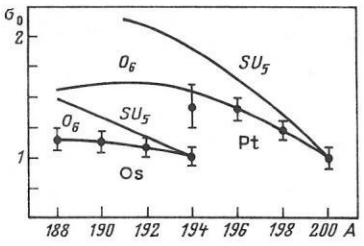

FIG. 19. Relative cross sections of the (t, p) reaction taking place to the ground state of the Os and Pt isotopes.[92]

In the interacting-boson model, the excited 0_2^+ and 2_1^+ states of deformed nuclei have a structure similar to single-phonon β and γ states. The wave functions of the following 0^+ states do not contain two-quasiparticle or single-phonon components. From the point of view of the microscopic approach, this model takes into account only the small fraction of two-quasiparticle states that occurs in the β- and γ-vibrational phonons. However, the experimental data on the quasiparticle structure of phonons obtained from nuclear reactions indicate large two-quasiparticle or single-phonon components in the wave functions of these states. A more accurate description of 0^+ excitations can be obtained in the microscopic quasiparticle–phonon model of the nucleus,[98] according to which the total contribution of the single-phonon components to the wave functions of the second and third excited states may reach 80% and more.

PAIRING CORRELATIONS AND MONOPOLE EXCITATIONS OF NUCLEI

Pairing correlations of superconducting type play a universal part in the structure of nuclei. The essence of the superfluid model[2] consists of systematic application of the pairing interaction to the description of nuclear properties. The ground state of an even–even nucleus with developed pairing is determined as the vacuum, $\alpha_k |0\rangle = 0$, of the quasiparticles corresponding to the generalized canonical transformation

$$\alpha_k = \sum_{\lambda} (u_{k\lambda} a_\lambda + v_{k\lambda} a_\lambda^+). \tag{51}$$

The coefficients $u_{k\lambda}$ and $v_{k\lambda}$ and the quasiparticle energies E_k are solutions of the Hartree–Fock–Bogolyubov system of equations

$$\left.\begin{aligned} E_k u_{k\lambda} &= \sum_{\lambda'} \{(h_{\lambda\lambda'} - \mu\delta_{\lambda\lambda'}) u_{k\lambda'} + \Delta_{\lambda\lambda'} v_{k\lambda'}\}; \\ -E_k v_{k\lambda} &= \sum_{\lambda'} \{(h_{\lambda\lambda'} - \mu\delta_{\lambda\lambda'}) v_{k\lambda'} + \Delta_{\lambda\lambda'} u_{k\lambda'}\}, \end{aligned}\right\} \tag{52}$$

where μ, the chemical potential, determines the number of particles of the given species, and h, the single-particle Hamiltonian, determines the representation, i.e., $h_{\lambda\lambda'} = e_\lambda \delta_{\lambda\lambda'}$. The pairing field is

$$\Delta_{\lambda\lambda'} = -\frac{1}{2} \sum_{\nu\nu'} \Gamma^{\xi}_{\lambda\lambda',\nu\nu'} \sum_k u_{k\nu} v_{k\nu'}, \tag{53}$$

where Γ^{ξ} is the effective interaction in the particle–particle channel.

The overwhelming majority of the calculations are made in the approximation of "constant" pairing:

$$\Gamma^{\xi}_{\lambda\bar{\lambda},\nu\bar{\nu}} = -G\delta_{\lambda\bar{\lambda}}\delta_{\nu\bar{\nu}}, \tag{54}$$

which is attractive on account of its simplicity. In this approximation, the system of equations (52) goes over into the equation of pairing correlations with a constant pairing field Δ, and the condition (53) becomes an equation for determining this constant. As was already noted in one of the pioneering studies,[99] the use of the interaction (54) is admissible only for the description of the ground state of the nucleus and the Fermi (quasiparticle) branch of excitations; for the boson branch, it is invalid. This is the case because the constant-pairing approximation breaks the nuclear symmetries, in particular the gauge symmetry,[59,100] which ensures conservation of the particle number.

In spherical nuclei, a correct microscopic description of the properties of the vibrational 2^+ and 3^- states requires allowance for the particle–particle forces on an equal footing with the particle–hole forces,[101] but the interaction (54) does not make a dynamical contribution to states with zero spin. Allowance for it in the problem of nuclear dipole resonance leads to pronounced unphysical effects in the photoabsorption cross sections.[102] The approximation (54) corresponds to zero angular momentum of a pair (monopole pairing), but in deformed nuclei this condition is too strong—it is necessary to have vanishing of only the projection of the pair angular momentum onto the symmetry axis.

The simplest methods of constructing effective two-particle interactions with allowance for the symmetry conditions are described in Refs. 103 and 104. For example, the corresponding condition makes it possible to augment the pairing interaction (54) by separable terms that, without changing the single-particle picture, restore its gauge invariance. Then there appears in the excitation spectrum of the nucleus a new branch of collective motion—T-odd fluctuations of the pairing.[59,80] These additional terms in the interaction represent multipole pairing, which was introduced independently into the theory phenomenologically in order to explain features in the cross sections of two-particle transfer reactions with excitation of the lowest collective states of both spherical[105] and deformed[106,107] nuclei. Simultaneously, the introduction of multipole pairing improves the description of the energy levels and transition probabilities for the lowest excited states of spherical nuclei.[108]

The simplest interaction corresponding to the requirement of translational and rotational invariance is

$$\Gamma^{\xi} = -g\delta(\mathbf{r} - \mathbf{r}') \tag{55}$$

with one universal constant g (Ref. 109) instead of the two constants $G_{n,p}$ for the neutrons and protons in the constant-pairing model. The locality of the interaction (55) automatically ensures gauge invariance of the theory when allowance is made for all its matrix elements that occur in the consistency condition (53). This leads to nondiagonality of the pairing field on the single-particle basis, a reflection of its multipole nature. The force constants for all multipolarities in (55) are the same, in agreement with the results of a phenomenological

TABLE XII. Dependence of the pairing field on the state.[110]

State	$\Delta_{\lambda\bar{\lambda}}$, MeV	Δ_k, MeV
1/2 [521]	0.932	1.019
7/2 [633]	0.951	1.019
5/2 [512]	0.987	0.926
5/2 [523]	0.928	1.190
7/2 [514]	0.983	1.158
1/2 [651]	1.015	0.858
5/2 [642]	1.017	1.110

analysis.[105] At the same time, each quasiparticle state is fragmented over single-particle states, in agreement with the observed spectroscopic factors of single-nucleon transfer reactions.[110] The nondiagonality and the strong dependence of the pairing field on the state in this approach eliminate the unphysical crowding of the single-quasiparticle states near the ground state of an odd nucleus characteristic of the traditional approach.[8] Table XII gives the diagonal components $\Delta_{\lambda\bar{\lambda}}$ of the pairing field and the effective parameters Δ_k as determined from the relation $E_k^2 = (e_k - \mu)^2 + \Delta_k^2$ using the calculated values E_k and μ in the ^{168}Er nucleus. The stronger dependence of Δ_k on the state due to the contribution to E_k of the nondiagonal components $\Delta_{\lambda\lambda'}$ agrees qualitatively with the results of phenomenological analysis of single-quasiparticle energies.[111] Analogous results are obtained in the model with projection with respect to the particle number.[112]

As has already been noted,[75] calculations for deformed nuclei made self-consistently with respect to the particle–hole channel revealed the need to go beyond the constant-pairing approximation. The self-consistent treatment of pairing (taking into account the invariance principles) made it possible to describe well the energy levels of the lowest 0^+ excitations in deformed nuclei in the rare-earth region with a single universal parameter of the quadrupole forces[113]:

$$\varkappa\,(0^+) = 61\,A^{-7/3}\ \text{MeV/F}^4, \tag{56}$$

this having a value close to the one obtained from the condition of consistency of the quadrupole interaction with the average-field potential that occurs in the Hamiltonian h. The interference of the pairing branch with the quadrupole vibrations leads to a large admixture of the pairing component in the wave functions of the lowest 0^+ states, in agreement with the results of other calculations[81,107] and the data of experiments on the excitation of these states in two-particle transfer reactions. At the same time, the probabilities of $E0$ and $E2$ transitions can be fairly well described without the introduction of effective charges,[113] as is demonstrated in Table XIII.

According to the estimates of Ref. 114, the most collectivized 0^+ state of the branch of coherent pairing fluctuations must lie in the region of the two-quasiparticle threshold ($E \approx 2\Delta$) and must be characterized by an anomalously small $E2$-transition probability; it must therefore have a large value of $X(E0/E2)$. Calculations in the model with self-consistent pairing[115] confirmed that in deformed nuclei with developed pairing the "X anomaly," discussed in the Introduction, is indeed associated with this branch of nuclear excitations. As can be seen from Fig. 20, calculations in the constant-pairing model do not give 0^+ states with large $X(E0/E2)$.

In the distorted-wave Born approximation for a direct single-step reaction mechanism the coherent properties of two-nucleon transfer cross sections are determined by the spectroscopic factors[61,116]:

$$\overset{\pm}{S}_n(A) = |\langle n,\ A|\overset{\pm}{T}|0,\ A \mp 2\rangle|^2, \tag{57}$$

TABLE XIII. Properties of low-lying monopole states of deformed nuclei.[113]

Nucleus	$E(0^+)$, MeV		$B(E2)$, $e^2\cdot F^4$		$\rho(E0;\ 0^+ - 0_1^+)$		$X(E0/E2)$	
	Theory	Experiment	Theory	Experiment	Theory	Experiment	Theory	Experiment
^{158}Dy	0.958	0.990	224	>77	0.16	>0.08	0.20	0.08 (3)
	1.708	1.665	9	—	0.13	—	3.01	—
	2.013	—	1	—	0.01	—	0.06	—
^{164}Er	1.246	1.246	352	>13	0.20	>0.02	0.22	0.14 (2)
	1.664	1.702	2	—	0.12	—	12.2	0.39 (6)
	1.960	1.766	215	—	0.19	—	0.33	0.64 (11)
	1.991	1.842	21	—	0.05	—	0.20	2.34 (70)
	2.117	2.173	22	—	0.02	—	0.05	0.88 (18)
^{168}Yb	0.936	1.156	1016	>1	0.47	>0.01	0.42	0.11 (2)
	1.188	1.197	387	<1	0.28	>0.04	0.39	0.51
	1.718	1.543	2	<1	0.10	>0.01	8.07	>3.1
	1.877	1.904	17	—	0.05	—	0.27	—
^{178}Hf	0.993	1.199	617	≲20	0.21	—	0.15	0.18 (2)
	1.571	1.434	213	270	0.16	—	0.25	0.11 (1)
	1.718	1.772	6	—	0.06	—	1.12	0.57 (16)
	1.850	1.817	12	—	0.03	—	0.13	—

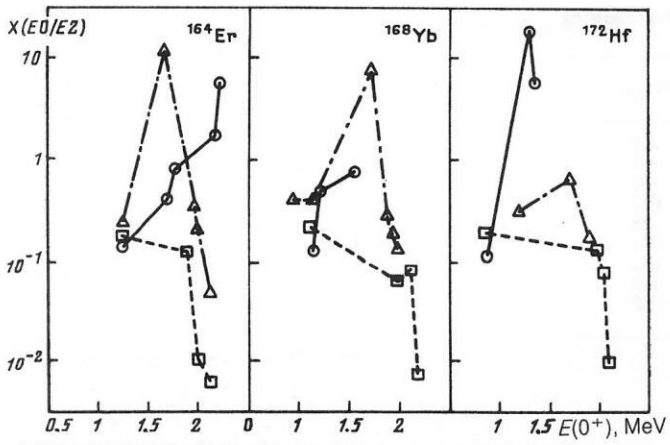

FIG. 20. The ratio $X(E0/E2)$ as a function of the excitation energy of the 0^+ level.[115] The open circles are the experimental values, the open triangles are the calculations in the model with self-consistent pairing, and the open squares are the calculations in the constant-pairing model.

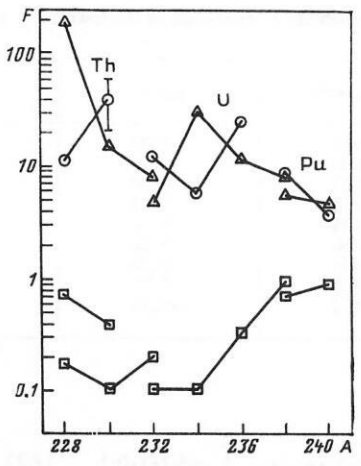

FIG. 21. Hindrance factors of α decay to the first excited 0^+ state.[120] The open circles are the experimental values, the open triangles are the calculations in the model with a mobile basis, and the open squares are the results of traditional calculations.

where $\overset{\pm}{T}$ are the operators of stripping or pickup of two particles. For reactions taking place to the ground state of the final nucleus, the symmetry property

$$\bar{S}_0(A) = \overset{+}{S}_0(A+2) \tag{58}$$

holds, and this is well satisfied in the experimental cross sections. In calculations, one usually ignores the difference between the properties of the ground states of neighboring nuclei. In the constant-pairing approximation (54) this leads to the well-known result

$$\overset{+}{S}_0^{(0)} = \bar{S}_0^{(0)} = \{2\Delta/G\}^2, \tag{59}$$

where Δ, the corresponding value of the pairing field, agrees with (58) only if the $\overset{\pm}{S}_0^{(0)}$ do not depend on A, a requirement that, in general, does not agree with the experimental data. The difference of the $\overset{\pm}{S}_0$ is due to the inhomogeneity of the single-particle spectrum near the Fermi surface and is particularly noted at the edges of the deformation region.

In the model with self-consistent pairing, the two branches of coherent pairing fluctuations, T-even and T-odd, lead to an asymmetry of the spectroscopic factors of reactions that take place with the excitation of monopole states of the nuclei.[110] Analogous results were obtained in the "pairing-plus-quadrupole-forces" model with projection with respect to the particle number[117] and in the model with a "mobile basis,"[118] which takes into account the change in the pairing field following excitation. The inclusion of additional T-odd components of the particle–hole interaction (spin-quadrupole,[79] for example) with adjustable parameters can bring these results into quantitative agreement with experiment, although the particle–particle channel must play the main part in forming the nuclear 0^+ states.

Calculations in the constant-pairing approximation (54) encounter serious difficulties in describing the hindrance factors of α decay to low-lying 0^+ states. It is well known that the observed rate of α decay to the first excited 0^+ state in heavy deformed nuclei is less than the rate of α decay to the ground state.[119] In contrast, the theoretical rates of α decay to the β-vibrational state, calculated in the traditional approach, are greater. Here, an important part is played by the condition of conservation of the average particle number in the dynamically deformed system.[120] This condition is satisfied by taking into account a residual interaction in the particle–particle channel, this corresponding to a change in the chemical potential μ following excitation. The hindrance factor of α decay to the excited 0^+ state is

$$F = \left\{\frac{\delta\Delta_n}{\Delta_n} + \frac{\delta\Delta_p}{\Delta_p}\right\}^{-2}, \tag{60}$$

where $\delta\Delta_{p,n}$ are the changes in the pairing field following excitation as calculated in the random-phase approximation. In Fig. 21, the results of the calculations are compared with the existing experimental data.

EXCITATION OF A NUCLEUS FOLLOWING DECAY OF A BOUND MUON

As is shown in Ref. 121, low-lying monopole states can be excited by the decay of a muon in a K orbital of a mesic atom. The calculation of the probability of this process depends strongly on the model chosen for the structure of the lowest nuclear 0^+ states. Therefore, the experimental investigation of this process, which has dependent value, is also of interest for theory.

The high energy of the electron produced as a result of the μ decay permits the conclusion that it leaves the region of the atom instantaneously and enables one to ignore interaction in the final state. In the "shake-off" approximation the probability of excitation of the nucleus, normalized to one decay event,

$$w_n = |\langle 0_n^+|V|0_1^+\rangle|^2/E^2(0_n^+), \tag{61}$$

is determined by the properties of the monopole states. The operator

TABLE XIV. Estimate of the probability of excitation of the lowest 0^+ states following muon decay.

Nucleus	$E(0^+)$, MeV	$\rho(E0)$	$w^{(0)} \cdot 10^6$
^{42}Ca	1.837	0.33	<1
^{72}Ge	0.690	0.10	5
^{72}Se	0.937	0.30	32
^{98}Sr	0.216	0.23	652
^{114}Cd	1.134	0.16	28
^{152}Sm	0.685	0.23	397
^{154}Gd	0.681	0.30	782
^{174}Hf	0.828	0.22	390
^{240}Pu	0.862	>0.13	>262

$$V = -e^2 \sum_p \left\{ \frac{1}{r_p} \int_0^{r_p} r^2 \varphi_K^2(r)\, dr + \int_{r_p}^{\infty} r \varphi_K^2(r)\, dr \right\} \qquad (62)$$

acts only on the protons, where $\varphi_K(r)$ is the radial part of the wave function of the muon in the K orbital of the mesic atom. It describes the Coulomb interaction of the muon with the protons of the nucleus with allowance for the penetration effect. When the muon decays, this interaction is switched off "instantaneously," and this leads to excitation of the nucleus.

The matrix elements of the operator V which occur in the probability (61) are like the corresponding quantities $\rho(E0)$.[115] This can be used to obtain a model-independent upper bound for the probabilities (61) from the experimental values of $\rho_n(E0)$ and $E(0_n^+)$:

$$w_n \leqslant w_n^{(0)} = \{e^2 R_0^2 \varphi_K^2(0)\, \rho_n(E0)\}^2 / 36 E^2(0_n^+). \qquad (63)$$

In Table XIV, this bound is given for the first excited 0^+ states of various nuclei. In the microscopic calculation of the probabilities (61) one must consider the question of the orthogonality of the wave functions of the monopole states, since only the spatial change of the potential (62) within the nucleus operates on excitation. Such a calculation[122] for 0_2^+ states gave a result close to the bound (63) and made it possible to follow the influence of the structure of higher monopole states on the excitation probabilities. Smallness of the probability of excitation of a nucleus following decay of a bound muon agrees with the fact that an experimental study of the $2s2p$ transition in the ^{68}Zn mesic atom did not reveal dynamical $E0$ excitation of the nucleus.[123]

At the present time, an experimental search is being made for excitation of nuclei following decay of bound muons. The experiment is arranged to detect γ rays of the nuclear transition from the excited 0^+ state in coincidence with fast electrons from the μ decay. The experiment must meet extremely stringent requirements on the resolution time; it must separate the prompt x-ray emission accompanying the atomic transitions of the muon from the nuclear γ rays, which are delayed by the muon lifetime. The choice of the target nucleus is dictated both by the estimate (63) and by the possibility of conversion de-excitation of the excited 0^+ level. Table XV considers the ratios of the probabilities $w_e(E0; 0_2^+ - 0_1^+)$ and $w_e(E2; 0_2^+ - 2_1^+)$ of conversion de-excitation of the 0_2^+ levels to the probability $w_\gamma(E2; 0_2^+ - 2_1^+)$ of radiative transition in two nuclei with very different charges Z. Elementary calculations using tables of conversion coefficients show that the 0_2^+ level in ^{152}Sm will be de-excited predominantly by γ rays, the 0_2^+ level in ^{232}U with approximately the same energy will be almost completely converted. As a result of these calculations, one must recognize Sm or Gd nuclei as the optimal choice for the target.

CONCLUSIONS

There is no doubt that it is important to obtain good quantitative agreement between the theoretical description and the experimental data, not only for the theory but also from the point of view of the planning of new experiments. Present-day models can explain nuclear properties in fairly wide ranges, indicate regions in which a significant advance in qualitative understanding is required, and identify problems suitable for detailed calculations. This is true in full measure for the problem of nuclear monopole excitations.

It has now been established that the formation of the excited 0^+ states of even–even nuclei may involve the participation of the following basic modes of nuclear motion. First, we have the particle–hole excitations characteristic of light nuclei, or two-quasiparticle excitations for nuclei with developed pairing. Typical of this mode are weak $E0$ transitions, reflecting the small polarization of the nucleus and the radial

TABLE XV. Probabilities of conversion and radiative de-excitation of nuclear 0_2^+ levels.

Nucleus	$E(0_2^+)$, MeV	$E(2_1^+)$, MeV	$X(E0/E2)$	$w_e(E2)/w_\gamma(E2)$	$w_e(E0)/w_\gamma(E2)$
^{152}Sm	0.685	0.122	0.11	0.01	0.02
^{232}U	0.695	0.048	0.17	0.02	0.96

redistribution of the charge following excitation. The residual interaction may lead to collectivization of the states of this type, when a large number of corresponding components contribute to the wave function. We must here mention giant monopole resonances and the branch of pairing vibrations. The coherence of these states is manifested accordingly in large amplitudes of the $E0$ transition and the transfer of a pair of particles to the ground state. The existing theory is capable of giving a completely adequate quantitative description of these states.

The more complicated $2p2h$ excitations are characteristic of light nuclei with $N \neq Z$ and nuclei with closed shells. Such excitations in the proton system lead to 0^+ states coupled to the ground states by $E0$ transitions with an amplitude of order ρ_0 ($E0$). The polarization of spherical nuclei of intermediate atomic mass following $2p2h$ excitations can be very appreciable, even changing the equilibrium shape. In this case, one observes in the spectrum a branch of intruder states, whose properties are analogous to those of the ground-state rotational band of the neighboring deformed nuclei. In this direction systematic self-consistent calculations, which would make it possible to clarify the details of the "development" of the nuclear deformation, would appear to be promising.

Monopole excitations can be associated with the occurrence or change of the relative motion of α clusters in nuclei. This mode is a consequence of short-range correlations in complicated particle–hole configurations ($4p4h$, for example) and is characterized in light nuclei by strong $E0$ transitions. Here, the theory is capable of giving a quantitative description in the framework of specific models.

At the macroscopic level, the monopole states are described by the vibrational model. Single-phonon 0^+ states are observed in deformed nuclei (coherent two-quasiparticle configurations); two-phonon states of quadrupole and octupole types are observed in spherical nuclei; and, finally, three-

TABLE AI. Observed energies of 0^+ levels and characteristics of $E0$ transitions to the ground states of even–even nuclei.

Nucleus	$E(0^+)$, MeV	$\rho(E0)$	$X(E0/E2)$
^{4}He	20.26	0.55 (9)	—
^{10}Be	6.18	0.22	—
^{12}C	7.655	0.72 (2)*	—
^{10}O	14.00	0.36 (8)	—
^{14}O	5.930	—	—
^{16}O	6.052	0.41 (1)*	—
	11.260	—	—
	12.050	0.48 (3)*	—
	14.035	0.41 (3)	—
^{18}O	3.632	0.38	—
		0.61 (7)	
	5.33	$\leqslant$0.45	—
^{24}Mg	6.432	0.55 (4)*	—
	8.85	—	—
	9.30	—	—
	10.10	—	—
	10.716	0.32 (6)	—
^{26}Mg	3.586	0.24 (2)	—
	4.965	—	—
^{28}Si	4.975	0.55 (4)*	—
	6.690	0.15 (8)	—
^{30}Si	3.788	0.10 (1)*	—
^{32}S	3.778	0.69 (7)	—
		0.13 (2)*	
^{34}S	3.915	0.10 (1)*	—
^{36}S	3.338	0.09	—
^{38}Ar	3.377	0.43 (4)	—
^{40}Ca	3.353	0.17 (3)*	—
	5.212	<0.06	—
^{42}Ca	1.837	0.33 (5)*	0.043 (4)
^{44}Ca	1.884	0.30 (2)*	—
^{46}Ca	2.423	—	—
^{48}Ca	4.272	0.10 (2)*	—
	5.459	—	—
^{54}Fe	2.561	$\leqslant$0.48	0.49 (8)
	4.292	0.28 (5)	0.65 (18)
^{56}Ni	3.952	—	—
^{58}Ni	2.942	0.0025 (3)	0.84 (18)
	3.531	0.28 (6)	0.47 (8)
^{60}Ni	2.285	0.03—0,17	0.027 (4)
	3.318	0.28 (8)	0.49 (8)
	3.588	>0.019	2.9 (5)
^{62}Ni	2.048	0.28 (8)	0.028 (5)
^{64}Zn	1.910	0.062 (4)	2.30 (25)
	2.609	0.089 (16)	0.03 (1)
^{66}Zn	2.373	>0.014	0.047 (8)
	3.106	—	5.0 (12)
^{68}Zn	1.656	0.083 (40)	0.033 (6)
^{70}Zn	1.069	0.051 (15)	0.0029 (6)
^{70}Ge	1.215	0.09 (1)	0.0042 (3)
	2.307	—	0.23 (6)

Continuation of Table AI

Nucleus	$E(0^+)$, MeV	$\rho(E0)$	$x(E0/E2)$
^{72}Ge	0.690	0.100 (6)*	—
	1.709	—	—
^{72}Se	0.937	0.304 (3)	—
		0.176 (60)	
^{74}Se	0.854	0.16 (2)	0.13 (2)
^{88}Sr	0.216	0.23 (2)	0.035
^{88}Zr	1.521	—	0.0051 (10)
^{90}Zr	1.752	0.058 (2)*	—
		0.0183 (4)	
	4.125	—	—
^{92}Zr	1.375	0.09 (1)	0.020 (2)
^{94}Zr	1.300	0.11 (1)	0.043 (4)
^{96}Zr	1.594	0.086 (2)	—
^{96}Mo	1.148	0.11 (2)	0.008 (2)
^{98}Mo	0.736	0.165 (15)	—
^{100}Mo	0.694	0.215 (28)	0.018 (1)
^{100}Ru	1.130	0.078	0.011 (1)
	1.741	—	0.6 (3)
^{102}Ru	0.944	0.092	0.013 (2)
^{102}Pd	1.592	0.07—0,10	$>$400
^{104}Pd	1.334	0.07 (2)	0.012 (4)
^{106}Pd	1.134	0.12 (2)*	0.016 (3)*
	1.56	—	—
	1.706	—	0.09 (3)
	2.001	—	45 (8)*
	2.278	—	0.17 (4)
	2.624	—	0.120 (25)
	2.877	—	0.07 (2)
	3.082	—	1.6 (5)
	3.162	—	0.9 (7)
	3.221	—	0.05 (1)
	3.320	—	0.15 (7)
^{112}Cd	1.224	0.19 (3)	0.026 (1)*
	1.432	0.022 (3)	1.0 (2)
^{114}Cd	1.134	0.16 (1)*	0.025 (1)*
	1.305	0.46 (6)*	18 (2)*
		0.036	
	1.860	—	0.012 (4)
	2.438	—	0.56 (5)
	2.554	—	0.58 (9)
^{112}Sn	2.191	$\leqslant$0.11	0.046 (8)
^{114}Sn	1.953	0.16 (5)	0.042 (8)
	2.156	$<$0.037	$<$0.01
^{116}Sn	1.757	0.066 (11)	0.023 (7)
			0.0086 (18)
	2.027	0.030 (3)	0.066 (11)
^{118}Sn	1.758	0.072 (10)*	0.0089 (8)*
	2.057	0.020—0,064	0.11 (1)*
	2.497	—	$<$0.035
^{120}Sn	1.875	0.051 (7)	0.0070 (18)
	2.160	$<$0.17	0.22 (5)
^{122}Sn	2.089	—	—
	2.191	—	0.046 (5)
^{124}Te	1.156	—	0.183
	1.657	—	0.067
			0.012
	1.883	—	$>$3.5
	2.390	—	$\geqslant$0.6
^{126}Te	1.396	—	0.259
^{130}Xe	1.794	—	6 (3)
	2.016	—	100 (50)
^{134}Ba	1.761	—	2.93 (38)
	2.337	—	$>$0.015
	2.379	—	0.0010 (2)
^{136}Ba	1.580	—	0.11 (2)
^{138}Ce	1.474	0.05	0.063 (9)
		0.15	
^{140}Ce	1.902	0.12 (2)	0.051 (8)
	3.017	—	0.17
^{142}Nd	2.217	0.13 (2)	—
^{144}Sm	1.67	$>$0.05	—
^{148}Sm	1.426	—	0.016 (8)
^{150}Sm	0.740	0.15 (2)*	0.015 (3)*
	0.829	—	0.22 (2)
	1.256	—	$\geqslant$0.11
^{152}Sm	0.685	0.23 (3)*	0.11 (2)
			0.067 (4)*
	1.083	$<$0.015	0.035 (17)
^{154}Sm	1.096	—	—
^{146}Gd	2.162	0.10 (1)	$>$0.02
	3.016	—	—
^{150}Gd	1.207	—	—
^{152}Gd	0.615	0.25 (15)	0.0060 (2)*
			0.012 (2)*

Continuation of Table AI

Nucleus	$E(0^+)$, MeV	$\rho(E0)$	$X(E0/E2)$
			0.047 (5)
	1.048	—	0.09 (2)*
			0.011 (3)
^{154}Gd	0.681	0.30 (1)*	0.09 (2)*
	1.182	—	—
^{156}Gd	1.049	0.41 (5)*	0.1
		0.20 (3)*	
	1.168	0.061 (19)	<0.018
	1.715	—	1.5 (3)
	1.851	—	0.17 (5)
^{158}Gd	1.196	—	—
^{156}Dy	0.674	—	>0.06
^{158}Dy	0.990	>0.077	0.08 (3)
^{160}Dy	1.280	—	0.27 (8)
	1.953	—	0.65
^{162}Dy	1.127	—	—
	1.400	<0.04	0.048 (4)
^{158}Er	0.806	—	0.036 (7)
^{160}Er	0.894	—	—
^{162}Er	1.087	—	0.30 (9)
	1.420	—	0.081 (74)
^{164}Er	1.246	>0.02	0.14 (2)*
			0.26 (7)
	1.417	—	0.14 (5)
	1.702	—	0.39 (6)
			0.069 (23)
	1.766	—	0.64 (11)*
	1.842	—	2.34 (70)
	2.173	—	0.88 (18)
			1.76 (25)
			4.5 (15)
	2.185	—	5.56 (184)
^{166}Er	1.460	—	0.037 (9)
^{168}Er	1.215	—	—
^{168}Yb	1.156	>0.0084	0.11 (2)*
	1.197	0.035—0,081	0.51
			>1.1
	1.340	—	—
	1.543	>0.0063	0.76
			>3.1
^{170}Yb	1.069	<0.007	0.003 (1)*
	1.229	0.14 (3)	0.088 (7)
			0.129 (16)
	1.480	—	0.96 (3)*
	1.566	—	0.93 (14)
			0.57 (6)*
^{172}Yb	1.043	0.048 (7)	0.028 (4)
	1.405	<0.16	2.81 (31)
	1.794	—	0.34 (4)
	1.895	—	0.10 (3)
^{174}Yb	1.149	—	—
	1.305	—	—
	1.487	—	<0.051
	1.884	—	<0.175
^{172}Hf	0.872	—	0.121 (18)*
	1.296	—	19 (4)*
	1.336	—	6.0 (7)*
^{174}Hf	0.828	0.220 (25)	0.18 (1)*
			>0.71
^{176}Hf	1.150	—	0.22 (5)*
	1.293	—	8.3 (10)*
^{178}Hf	1.199	—	0.18 (2)*
			0.28 (3)
	1.237	—	—
	1.434	—	0.11 (1)*
			0.066 (7)
			>0.15
	1.444	—	0.54 (3)*
	1.772	—	0.57 (16)
^{180}W	0.908	0.03 (1)*	0.061
			0.2
^{182}W	1.135	—	—
^{184}W	1.004	0.0019 (4)	0.006 (3)
	1.285	—	—
^{186}W	0.882	—	—
^{188}Os	1.086	⩽0.022	<0.0035
	1.478	—	0.0072
	1.704	—	1.70
			4 (1)
	1.765	—	0.19 (3)*
	1.825	—	0.15
			0.7 (2)
^{190}Os	0.911	—	—

Continuation of Table AI

Nucleus	$E(0^+)$, MeV	$\rho(E0)$	$X(E0/E2)$
^{184}Pt	0.493	—	0.008 (3)
^{186}Pt	0.472	—	0.0065 (20)
^{188}Pt	0.799	—	0.0090 (15)
^{190}Pt	0.922	—	0.0062 (12)
^{192}Pt	1.195	—	0.022 (3)
^{194}Pt	1.267	—	0.0074 (7)*
	1.479	—	0.44 (6)
	1.547	—	0.020 (4)
	1.890	—	—
	2.086	—	5.6 (3)
	2.164	—	1.5 (3)
	2.357	—	>1.2
^{196}Pt	1.135	—	<0.005
	1.403	—	0.092
	1.823	—	<0.03
	1.918	—	0.060
^{206}Pb	1.166	0.031 (4)*	>1.6
^{208}Pb	4.882	—	—
^{208}Po	1.272	0.030—0.037	>0.7
^{212}Po	1.801	0.037 (3)*	—
^{214}Po	1.415	0.036 (1)	—
^{228}Th	0.831	—	0.83
^{230}Th	0.636	—	0.22 (10)
^{232}Th	0.730	—	0.12 (1)
^{232}U	0.695	—	0.17 (4)
^{234}U	0.810	—	0.50 (8)
^{236}U	0.919	—	—
^{238}U	0.994	—	0.20 (6)
	2.558	0.00003	0.32 (11)
^{238}Pu	0.942	—	0.24
			0.63 (20)
	1.229	—	0.13
^{240}Pu	0.862	0.13—0.30	0.05 (1)
^{244}Cm	0.985	—	1.5 (2)
^{250}Cf	1.154	—	0.27 (3)
	1.267	—	2.5 (3)

*Estimated values.

phonon states are observed in transitional nuclei. The nonadiabaticity of the surface vibrations leads to appreciable anharmonicity in the nuclear spectra, without allowance for which it is impossible to obtain a quantitative description. The first step in this direction is the phenomenological interacting-boson model. A microscopic calculation of the parameters of this model on the basis of a self-consistent approach would be of very great interest.

The experimental investigation of monopole excitations encounters a number of specific difficulties due to the comparatively weak excitation of 0^+ levels, the small values of the $E0/E2$ branching ratio, and other neglected reaction channels. The main sources of the large uncertainties in the experimental information about $E0$ transitions are the inadequate energy resolution of the spectrometers, the use of incomplete or incorrect decay schemes, and the use of estimates (instead of measurements) of $B(E2)$ or other matrix elements in the calculation of $\rho(E0)$ and $X(E0/E2)$. It is to be hoped that the development of experimental methods will give qualitatively new information about monopole excitations of nuclei and stimulate further theoretical investigations in this direction.

We should like to thank I. A. Kondurov for constant interest and support. We are grateful to N. I. Pyatov for interest in this work and helpful discussions, and also to the participants of the seminars at which this work was reported for friendly criticism, which we have attempted to take into account.

APPENDIX. ESTIMATED EXPERIMENTAL DATA

The most complete compilation of experimental data on 0^+ states and $E0$ transitions in even–even nuclei is kept, together with the source, on magnetic tapes at the Data Center of the Leningrad Institute of Nuclear Physics and is constantly updated.[11] We give here tables of estimated data based on this information (up to the middle of 1985), including energy levels, matrix elements of $E0$ transitions, and the ratios $X(E0/E2)$. In Table AI we give the energies of the 0^+ levels and the characteristics of $E0$ transitions to the ground state. As a rule, nuclei for which only the energies of the 0^+ levels have been determined experimentally and there is no information on the monopole transitions have not been included in Table AI. Also omitted are certain 0^+ levels whose decay characteristics have not been determined. Data on $E0$ transitions between excited 0^+ states or states with nonvanishing spins are given in Table AII.

The experimental information was evaluated in accordance with the generally adopted prescription. Individual ex-

TABLE AII. Characteristics of $E0$ transitions between excited states of even–even nuclei.

Nucleus	I^π	E_1, MeV	ΔE, MeV	$\rho(E0)$	$X(E0/E2)$
^{112}Cd	0^+	1.432	0.209	0.09	—
^{114}Cd	2^+	1.209	0.651	<0.09	<0.01
	0^+	1.305	0.171	0.020 (1)*	—
	2^+	1.364	0.806	0.24 (2)*	>30
			0.154	0.18 (1)*	0.032 (6)
	4^+	1.732	0.449	0.057	0.12 (2)
	2^+	1.842	1.284	—	<0.2
			0.633	0.12	0.71 (8)
			0.478	—	<0.014
	4^+	1.932	0.648	—	0.057 (22)
			0.200	—	<0.001
	2^+	2.048	0.838	—	<0.09
			0.206	—	<0.6
	4^+	2.152	0.869	—	<0.11
			0.420	—	<0.01
			0.220	—	<0.01
	3^+	2.204	0.340	—	0.052 (10)
	2^+	2.219	1.661	—	<0.3
			0.855	—	<0.07
^{114}Sn	0^+	2.156	0.203	<0.36	0.9 (3)
^{116}Sn	0^+	2.027	0.271	0.32 (4)	7.4 (12)
^{118}Sn	0^+	2.057	0.299	0.10—0,37	3.4 (15)
^{120}Sn	0^+	2.160	0.285	<1.14	8.0 (30)
^{124}Te	2^+	1.325	0.723	—	0.059
	0^+	1.883	0.226	—	5
	4^+	1.957	0.709	—	1.04
	2^+	2.039	1.437	—	0.21
			0.714	—	0.094
	2^+	2.092	1.490	—	5.16
	2^+	2.183	1.581	—	2.11
	2^+	2.323	1.721	—	7.10
^{144}Nd	2^+	1.561	0.864	—	0.25
^{146}Sm	2^+	2.103	1.356	—	0.13 (5)
	2^+	2.156	1.409	—	0.27 (14)
	6^+	2.223	0.411	—	0.025 (10)
	4^+	2.532	1.151	—	0.076 (22)
^{148}Sm	4^+	1.733	0.553	—	0.014 (7)
	4^+	1.895	0.715	—	>0.085
	4^+	2.327	1.147	—	0.071 (66)
^{150}Sm	2^+	1.046	0.712	0.22 (7)	0.05
	2^+	1.194	0.860	0.047	—
^{152}Sm	2^+	0.810	0.688	0.25 (2)*	0.43 (3)*
					0.090 (10)
	4^+	1.023	0.657	0.24 (5)*	0.66 (21)
	0^+	1.083	0.398	<0.09	—
	2^+	1.086	0.964	0.029 (4)	—
	4^+	1.372	1.006	0.09 (4)	—
	8^+	1.666	0.541	0.205 (60)	—
	10^+	2.103	0.495	0.28 (10)	—
^{150}Gd	2^+	1.519	0.880	0.105 (18)	0.062 (8)
	4^+	1.700	0.412	—	0.010 (10)
^{152}Gd	2^+	0.931	0.586	—	0.061 (11)
	4^+	1.282	0.527	—	0.234 (23)
	2^+	1.318	0.973	—	0.088 (11)
			0.387	—	0.31 (8)
	2^+	1.862	0.544	—	0.93 (18)
^{154}Gd	2^+	0.816	0.693	0.29 (2)*	0.43 (2)*
	2^+	0.996	0.873	0.062 (9)	—
	4^+	1.048	0.676	0.19 (6)*	0.45 (10)*
	4^+	1.265	0.893	0.07 (3)	—
	6^+	1.368	0.650	0.25 (2)*	0.34 (8)
	8^+	1.756	0.612	$\geqslant 0.20$	0.48 (15)
	10^+	2.194	0.557	—	0.27 (15)
^{156}Gd	2^+	1.130	1.040	0.44 (12)	0.19 (5)
				0.23 (5)*	0.52 (9)*
	2^+	1.258	1.168	<0.04	—
	4^+	1.298	1.010	0.22 (3)	0.20 (4)
					0.69 (16)
	4^+	1.462	1.174	<0.12	—
	6^+	1.540	0.956	—	0.18 (8)
	2^+	1.828	0.674	—	1.2
	8^+	1.848	0.883	—	0.05—0,08
	3^+	1.916	0.668	—	1.0
	10^+	2.220	0.804	—	0.06 (3)
^{158}Gd	2^+	1.260	1.180	0.027 (14)	—
	2^+	1.517	1.438	0.16 (6)	—
	4^+	1.667	1.406	<0.18	—
^{156}Dy	2^+	0.829	0.691	—	0.15 (2)*
	2^+	0.891	0.753	—	0.032 (15)
	4^+	1.088	0.684	—	0.20 (1)*
	4^+	1.161	0.757	—	0.045 (12)
	6^+	1.437	0.666	—	0.16 (4)
	6^+	1.525	0.754	—	0.085 (26)

Continuation of Table AII

Nucleus	I^π	E_1, MeV	ΔE, MeV	$\rho(E0)$	$X(E0/E2)$
	8^+	1.859	0.643	—	0.209 (35)
	8^+	1.957	0.741	—	0.045 (43)
	10^+	2.316	0.591	—	0.181 (41)
^{158}Dy	2^+	1.085	0.896	—	$>$0.05
	4^+	1.280	0.963	—	0.07 (3)
^{160}Dy	2^+	0.966	0.879	0.007 (4)	0.0008 (50)
^{164}Dy	2^+	0.762	0.689	—	0.000023 (5)
	4^+	0.916	0.674	—	0.000011 (1)
	6^+	1.154	0.653	—	0.000005 (1)
^{164}Er	2^+	1.315	1.223	—	0.29 (5)*
	4^+	1.470	1.170	—	1.01 (48)
	2^+	1.484	1.392	—	0.87 (25)
	0^+	1.702	0.456	—	$>$0.09
	0^+	1.766	0.520	—	$>$0.05
	2^+	1.788	1.696	—	0.30 (3)
					0.64 (19)
			0.473	—	0.11 (3)
	2^+	1.833	1.741	—	0.89 (34)
	2^+	1.911	1.819	—	0.65 (21)
	2^+	1.955	1.863	—	0.13 (6)
					0.49 (16)
	0^+	2.173	0.927	—	$>$2.9
			0.407	—	$>$0.017
	2^+	2.278	2.187	—	0.052 (10)
					13.9 (59)
			0.963	—	0.70 (31)
			0.795	—	0.47 (22)
^{170}Yb	2^+	1.139	1.054	$<$0.022	—
	2^+	1.146	1.061	$\leqslant$0.01	$\leqslant$0.0017
	2^+	1.316	1.221	0.14 (5)	0.100 (12)
	2^+	1.534	1.449	—	0.64 (8)
	2^+	1.634	1.549	—	0.101 (13)
^{172}Yb	2^+	1.118	1.040	0.038 (6)	0.075 (20)
	4^+	1.287	1.026	0.021 (16)	0.020 (4)*
	2^+	1.466	1.388	0.022 (18)	0.107 (10)
	2^+	1.477	1.399	—	0.015 (3)
	4^+	1.658	1.397	0.049 (20)	0.029 (20)
	2^+	1.849	1.771	—	0.12 (3)
	2^+	1.956	1.878	—	0.09 (3)
^{174}Hf	2^+	0.900	0.809	0.23 (2)	—
	4^+	1.062	0.765	0.20 (3)	—
	6^+	1.308	0.699	0.22 (3)	—
^{176}Hf	2^+	1.226	1.138	—	0.9 (3)
					0.14 (6)
	2^+	1.379	1.291	—	1.0
					0.16
	4^+	1.390	1.100	—	0.10 (3)
	6^+	1.629	1.032	—	0.10 (2)
	8^+	1.933	0.935	—	0.09 (4)
	10^+	2.295	0.814	—	0.04 (2)
^{178}Hf	2^+	1.277	1.183	—	1.56 (15)
					0.34 (5)
	4^+	1.450	1.144	—	0.17 (1)
	2^+	1.496	1.402	—	0.76 (4)
					0.44 (3)
	2^+	1.562	1.468	—	0.23 (2)
	6^+	1.731	1.099	—	0.16 (2)
	2^+	1.818	1.724	—	0.53 (4)
	4^+	1.956	1.650	—	0.37 (4)
^{182}W	2^+	1.222	1.121	0.019 (11)	0.0016 (11)
	2^+	1.258	1.157	0.049 (6)	0.090 (24)*
	4^+	1.442	1.113	—	0.011 (5)
^{184}W	2^+	0.904	0.793	$\leqslant$0.021	$\leqslant$0.0017
	2^+	1.121	1.010	0.044 (12)	0.095 (19)
^{188}Os	2^+	0.633	0.478	0.022 (10)	—
^{190}Os	2^+	0.557	0.371	$<$0.030*	0.000 04 (17)
^{184}Pt	2^+	0.841	0.679	—	$\geqslant$0.13
					0.012 (2)
^{186}Pt	2^+	0.799	0.607	—	0.014 (2)
^{188}Pt	2^+	0.606	0.340	—	$\leqslant$0.0011
	2^+	1.115	0.849	—	$\geqslant$0.50*
^{190}Pt	2^+	0.598	0.302	—	$\leqslant$0.0001
	2^+	1.204	0.908	—	0.071 (28)
^{192}Pt	2^+	0.612	0.296	0.016 (1)*	0.000013 (10)
				0.004 (5)	
	2^+	1.439	1.123	—	$\geqslant$0.25
	2^+	1.576	1.260	—	0.025 (5)
^{194}Pt	2^+	0.622	0.293	0.0109 (66)	—
	2^+	1.512	1.183	—	0.022 (9)
			0.890	—	0.022 (15)
	2^+	1.623	1.294	—	0.24 (9)
			1.101	—	0.024 (12)
	2^+	2.312	1.983	—	2.1 (7)

Continuation of Table AII

Nucleus	I^π	E_1, MeV	ΔE, MeV	$\rho(E0)$	$X(E0/E2)$
^{196}Pt	2^+	0.689	0.333	0.039 (7)	—
				<0.016*	
^{186}Hg	2^+	0.621	0.216	—	0.027 (4)
^{188}Hg	2^+	0.881	0.468	—	0.016 (3)
^{198}Hg	2^+	1.088	0.676	0.21—0.42	>0.87
^{228}Th	2^+	1.154	0.185	0.11 (2)	—
^{232}Th	2^+	0.774	0.725	0.37 (6)	—
^{238}U	2^+	1.037	0.991	0.097	
				0.43 (6)	

*Estimated values.

perimental data are transferred without change. Independent experimental values x_i of any quantity with overlapping errors were averaged: $\bar{x} = \sum_{i=1}^{N} x_i/N$. The new error was determined statistically: $\Delta x = \left\{ \sum_{i=1}^{N} (x_i - \bar{x})^2/N \right\}^{1/2}$. In the tables, estimated values are identified by an asterisk. Nonoverlapping experimental data are transferred to the tables unchanged, the chronological order being observed, i.e., the latest value is given last. The energies of the levels and transitions are, as a rule, determined with an error not greater than 1 keV, and they therefore appear in the tables without an error. When this is not the case, the reliable significant figures are retained.

[1] L. A. Borisoglebskiĭ, Usp. Fiz. Nauk **81**, 271 (1963) [Sov. Phys. Usp. **6**, 715 (1964)].
[2] B. S. Dzelepov and S. A. Shestopalova, in: Nuclear Structure, IAEA, Vienna (1968), p. 39.
[3] N. I. Pyatov, Preprint R4-5422 [in Russian], JINR, Dubna (1970); N. I. Pyatov, Problemy sovremennoĭ yadernoĭ fiziki (Problems of Modern Nuclear Physics), Nauka, Moscow (1972), pp. 141–157.
[4] A. V. Aldushchenkov and N. A. Voinova, Nucl. Data Tables **A11**, 299 (1972).
[5] N. A. Voinova, Preprint No. 230 [in Russian], Leningrad Institute of Nuclear Physics, Leningrad (1976); Publication INDC(CCP)-93/N, IAEA, Vienna (1976).
[6] J. Kantele, Preprint RR-18/81, Jyvaskyla (1981).
[7] J. Lange, K. Kumar, and J. H. Hamilton, Rev. Mod. Phys. **54**, 119 (1982).
[8] A. Bohr and B. R. Mottelson, Nuclear Structure, Vol. 2, Benjamin, Reading, Mass. (1975) [Russian translation published by Mir, Moscow (1977)].
[9] J. M. Eisenberg and W. Greiner, *Nuclear Theory, Vol. 1, Nuclear Models* (North–Holland, Amsterdam 1970) [Russian translation published by Atomizdat, Moscow (1975)].
[10] V. G. Solov'ev, Teoriya slozhnykh yader, Nauka, Moscow (1971); English translation: V. G. Soloviev, *Theory of Complex Nuclei* (Pergamon Press, Oxford 1976).
[11] N. A. Voinova-Eliseeva and I. A. Mitropol'skiĭ, Preprints Nos. 1104 and 1105 [in Russian], Leningrad Institute of Nuclear Physics, Leningrad (1985).
[12] J. Schirmer, D. Habs, R. Kroth *et al.*, Phys. Rev. Lett. **53**, 1897 (1984).
[13] E. L. Church and J. Weneser, Phys. Rev. **103**, 1035 (1956).
[14] R. B. Begzhanov and V. M. Belen'kiĭ, Struktura yadra (Nuclear Structure), Fan, Tashkent (1969), pp. 256–293; R. S. Hager and E. C. Seltzer, Nucl. Data Tables **A6**, 1 (1969).
[15] J. O. Rasmussen, Nucl. Phys. **19**, 85 (1960).
[16] O. Bohigas, A. M. Lane, and J. Martorell, Phys. Rep. **51**, 267 (1979).
[17] B. N. Belyaev, S. S. Vasilenko, G. I. Karazhanova, and A. I. Pautov, Izv. Akad. Nauk SSSR Ser. Fiz. **42**, 1928 (1978).
[18] N. Vinh-Mau and G. E. Brown, Phys. Lett. **1**, 36 (1962).
[19] B. H. Wildenthal, J. B. McGrory, E.C. Halbert, and H.D. Graber, Phys. Rev. C **4**, 1708 (1971).
[20] J. B. McGrory and B. H. Wildenthal, Phys. Rev. C **7**, 974 (1973).
[21] S. LaFrance, H. T. Fortune, S. Mordechai, and R. Middleton, J. Phys. G **5**, L59 (1979).
[22] P. K. Rath, H. Müther, A. Polls *et al.*, Nucl. Phys. **A427**, 511 (1984).
[23] D. H. Gloeckner and R. D. Lawson, Phys. Lett. **53B**, 313 (1974).
[24] A. I. Baz', Yu. T. Grin', V. F. Demin, and M. V. Zhukov, Fiz. Elem. Chastits At. Yadra **3**, 275 (1972) [Sov. J. Part. Nucl. **3**, 137 (1972)].
[25] Yu. F. Smirnov and K. V. Shitikova, Fiz. Elem. Chastits At. Yadra **8**, 847 (1977) [Sov. J. Part. Nucl. **8**, 344 (1977)].
[26] D. M. Brink, in: Struktura slozhnykh yader (Structure of Complex Nuclei; Russian translation), Atomizdat, Moscow (1966), p. 111.
[27] K. Wildermuth and Y. C. Tang, *A Unified Theory of the Nucleus* (Academic Press, New York, 1977) [Russian translation published by Mir, Moscow (1980)].
[28] B. I. Barts, Yu. L. Bolotin, E. V. Inopin, and V. Yu. Gonchar, Metod Khartri–Foka v teorii yadra (The Hartree–Fock Method in Nuclear Theory), Naukova Dumka, Kiev (1982).
[29] V. Yu. Gonchar, E. V. Inopin, V. E. Mitroshin, and V. N. Tarasov, Preprint No. 1068 [in Russian], Leningrad Institute of Nuclear Physics, Leningrad (1985).
[30] H. W. Fulbright, Ann. Rev. Nucl. Part. Sci. **29**, 161 (1979).
[31] V. B. Subbotin, V. M. Semjonov, K. A. Gridnev, and E. F. Hefter, Phys. Rev. C **28**, 1618 (1983).
[32] P. Halse, J. P. Elliot, and J. A. Evans, Nucl. Phys. **A417**, 301 (1984).
[33] G. M. Lederer and V. S. Shirley, *Tables of Isotopes* (Wiley, New York, 1978).
[34] M. Bernas, Ph. Dessagne, M. Langevin *et al.*, Phys. Lett. **113B**, 279 (1982).
[35] J. Speth, E. Werner, and W. Wild, Phys. Rep. **33**, 127 (1977).
[36] É. E. Sapershteĭn, S. A. Fayans, and V. A. Khodel', Fiz. Elem. Chastits At. Yadra **9**, 221 (1978) [Sov. J. Part. Nucl. **9**, 91 (1978)]; V. A. Khodel and E. E. Saperstein, Phys. Rep. **92**, 183 (1982).
[37] J. Speth and J. Wambach, Nucl. Phys. **A347**, 389 (1980).
[38] J. Speth, L. Zamick, and P. Ring, Nucl. Phys. **A232**, 1 (1974); P. Ring and J. Speth, Nucl. Phys. **A235**, 315 (1974).
[39] K. Heyde, P. Van Isacker, M. Waroquier *et al.*, Phys. Rep. **102**, 291 (1983).
[40] P. Van Duppen, E. Coenen, and K. Deneffe *et al.*, Phys. Lett. **154B**, 354 (1985).
[41] P. Van Duppen, E. Coenen, K. Deneffe, *et al.*, Phys. Rev. Lett. **52**, 1974 (1984).
[42] J. Speth and A. Van der Woude, Rep. Prog. Phys. **44**, 719 (1981); F. E. Bertrand, Nucl. Phys. **A354**, 129 (1981).
[43] D. H. Youngblood, P. Bogucki, J. D. Bronson *et al.*, Phys. Rev. C **23**, 1997 (1981).
[44] J. P. Blaizot, D. Gogny, and B. Grammaticos, Nucl. Phys. **A265**, 315 (1976).
[45] A. F. Mezentsev, Yu. P. Smirnov, O. I. Sumbaev *et al.*, Izv. Akad. Nauk SSSR Ser. Fiz. **30**, 1167 (1966).
[46] K. Goeke and B. Castel, Phys. Rev. C **19**, 201 (1979).
[47] J. P. Blaizot and D. Gogny, Nucl. Phys. **A284**, 429 (1977).
[48] J. Bartel, P. Quentin, M. Brack *et al.*, Nucl. Phys. **A386**, 79 (1982).
[49] J. Treiner, H. Krivine, O. Bohigas, and J. Martorell, Nucl. Phys. **A371**, 253 (1977).
[50] M. B. Zhalov and L. A. Sliv, Preprint No. 710 [in Russian], Leningrad

Institute of Nuclear Physics, Leningrad (1981).
[51] R. A. Broglia and P. F. Bortignon, Phys. Lett. **101B**, 135 (1981); P. F. Bortignon and R. A. Broglia, Phys. Lett. **102B**, 303 (1981).
[52] J. S. Dehesa, S. Krewald, J. Speth, and A. Faessler, Phys. Rev. C **15**, 1858 (1977).
[53] V. C. Soloviev, Nukleonika **23**, 1149 (1978).
[54] C. Y. Wong, Nucl. Data **A4**, 271 (1968).
[55] M. A. J. Mariscotti, D. R. Bes, S. L. Reich *et al.*, Nucl. Phys. **A407**, 98 (1983).
[56] E. E. Berlovich, S. S. Vasilenko, and Yu. N. Novikov, Vremena zhizni vozbuzhdennykh sostoyaniĭ atomnykh yader (Lifetimes of Excited Nuclear States), Nauka, Leningrad (1972).
[57] D. Bes and R. Sorensen, Adv. Nucl. Phys. **2**, 129 (1969).
[58] D. Bes and R. A. Broglia, Nucl. Phys. **80**, 289 (1966).
[59] S. T. Belyaev, Yad. Fiz. **4**, 936 (1966) [Sov. J. Nucl. Phys. **4**, 671 (1967)].
[60] S. T. Belyaev and B. A. Rumiantsev, Phys. Lett. **30B**, 444 (1969).
[61] R. A. Broglia, O. Hansen, and C. Riedel, Adv. Nucl. Phys. **6**, 287 (1973).
[62] V. B. Telitsyn, Ch. Stoyanov, and A. I. Vdovin, Yad. Fiz. **24**, 31 (1976) [Sov. J. Nucl. Phys. **24**, 16 (1976)].
[63] V. G. Solov'ev, Fiz. Elem. Chastits At. Yadra **9**, 860 (1978) [Sov. J. Part. Nucl. **9**, 343 (1978)].
[64] D. Dambasuren, A. I. Vdovin, and Ch. Stoyanov, Preprint R4-8778 [in Russian], JINR, Dubna (1975).
[65] A. S. Davydov, Vozbuzhdennye sostoyaniya atomnykh yader (Excited Nuclear States), Atomizdat, Moscow (1967).
[66] K. Kumar and M. Baranger, Nucl. Phys. **A92**, 608 (1967).
[67] K. Kumar and M. Baranger, Nucl. Phys. **A110**, 529 (1968).
[68] K. E. G. Löbner, M. Vetter, and V. Hönig, Nucl. Data Tables **A7**, 495 (1970).
[69] R. B. Begzhanov, V. M. Belen'kiĭ, edited by S. R. Abdurakhmanov, and V. K. Usharov, Sovremennye, modeli chetno-chetnykh yader (Modern Models of Even–Even Nuclei), Uzbekistan, Tashkent (1973).
[70] M. Sakai, At. Data Nucl. Data Tables **31**, 399 (1984).
[71] K. Hara, Nucl. Phys. **46**, 385 (1963).
[72] K. Kumar and M. Baranger, Nucl. Phys. **A122**, 273 (1968).
[73] V. G. Soloviev and N. Yu. Shirikova, Z. Phys. A **301**, 263 (1981); F. Meliev *et al.*, in Yadernaya spektroskopiya i struktura atomnykh yader. Tezisy dokladov 35 Soveshchaniya (Nuclear Spectroscopy and Nuclear Structure. Abstracts of Papers at the 35th Symposium), Nauka, Leningrad (1985), p. 164.
[74] L. K. Peker and J. H. Hamilton, *Future Directions in Studies of Nuclei Far from Stability* (North–Holland, Amsterdam, 1980), pp. 323–337.
[75] V. V. Pal'chik and N. I. Pyatov, Yad. Fiz. **32**, 924 (1980); **33**, 637 (1981) [Sov. J. Nucl. Phys. **32**, 476 (1980); *ibid* **33**, 333 (1981)].
[76] B. L. Birbrair, N. A. Voinova, and N. S. Smirnova, Nucl. Phys. **A251**, 169 (1975).
[77] B. Silvestre-Brac and R. Piepenbring, Z. Phys. A **272**, 89 (1975).
[78] K. M. Zheleznova, N. I. Pyatov, and M. I. Cherneĭ, Izv. Akad. Nauk SSSR Ser. Fiz. **31**, 550 (1967); S. K. Abdulvagabova, S. P. Ivanova, and N. I. Ryatov, Yad. Fiz. **16**, 1209 (1972) [Sov. J. Nucl. Phys. **16**, 865 (1973)]; S. K. Abdulvagabova, Izv. Akad. Nauk SSSR Ser. Fiz. **37**, 1007 (1973).
[79] S. K. Abdulvagabova, V. B. Telitsyn, and G. Shul'ts, Izv. Akad. Nauk SSSR Ser. Fiz. **39**, 1701 (1975).
[80] B. V. Rumyantsev and V. B. Telitsyn, Yad. Fiz. **15**, 690 (1972) [Sov. J. Nucl. Phys. **15**, 387 (1972)].
[81] D. Zawischa, J. Speth, and D. Pal, Nucl. Phys. **A311**, 445 (1978).
[82] G. Gneuss, U. Mosel, and W. Greiner, Phys. Lett. **31B**, 269 (1978); G. Gneuss and W. Greiner, Nucl. Phys. **A171**, 449 (1971).
[83] R. A. Meyer, R. D. Griffioen, J. Graber Lefler, and W. B. Walters, Phys. Rev. C **14**, 2024 (1976).
[84] H. F. DeVries and P. J. Brussaard, Z. Phys. A **286**, 1 (1978).
[85] K. Takada and S. Tazaki, Nucl. Phys. **A395**, 165 (1983).
[86] K. J. Weeks, T. Tamura, T. Udagawa, and F. J. W. Hahne, Phys. Rev. C **24**, 703 (1981).
[87] J. B. Hamilton, A. V. Ramayya, W. T. Pinkston *et al.*, Phys. Rev. Lett. **32**, 239 (1974).
[88] R. B. Piercey, J. H. Hamilton, R. Soundranayagam *et al.*, Phys. Rev. Lett. **47**, 1514 (1981).
[89] G. Wenes, P. Van Isacker, M. Waroquier *et al.*, Phys. Rev. C **23**, 2291 (1981).
[90] K. Heyde, P. Van Isacker, J. Moreau, and M. Waroquier, Preprint LVK-84-01, Gent (1984).
[91] M. Carchidi and H. T. Fortune, Phys. Rev. C **31**, 853 (1985); H. T. Fortune and M. Carchidi, J. Phys. G **11**, L193 (1985).
[92] R. F. Casten, Nucl. Phys. **A347**, 173 (1980).
[93] R. V. Jolos, I. Kh. Lemberg, and V. M. Mikhaĭlov, Fiz. Elem. Chastits At. Yadra **16**, 280 (1985) [Sov. J. Part. Nucl. **16**, 121 (1985)].
[94] J. N. Ginocchio and M. W. Kirson, Nucl. Phys. **A350**, 31 (1980); A. Klein, C. T. Li, and M. Vallieres, Phys. Scr. **25**, 452 (1982).
[95] K. Heyde, P. Van Isacker, M. Waroquier *et al.*, Phys. Rev. C **25**, 3160 (1982).
[96] R. V. Jolos and V. Rybarska, Fiz. Elem. Chastits At. Yadra **3**, 739 (1972) [Sov. J. Part. Nucl. **3**, 377 (1973)]; R. V. Jolos and D. Janssen, Fiz. Elem. Chastits At. Yadra **8**, 330 (1977) [Sov. J. Part. Nucl. **8**, 138 (1977)].
[97] O. K. Vorov and V. G. Zelevinskiĭ, Yad. Fiz. **37**, 1392 (1983) [Sov. J. Nucl. Phys. **37**, 830 (1983)].
[98] V. G. Solov'ev, Pis'ma Zh. Eksp. Teor. Fiz. **40**, 398 (1984) [JETP Lett. **40**, 1216 (1984)].
[99] N. N. Bogolyubov, V. V. Tolmachev, and D. V. Shirkov, Novyĭ metod v teorii sverkhprovodimosti, USSR Academy of Sciences, Moscow (1958); English translation: A New Method in the Theory of Superconductivity, Consultants Bureau, New York (1959).
[100] S. T. Belyaev, Phys. Lett. **28B**, 365 (1969).
[101] B. L. Birbrair, K. I. Erokhina, and I. Kh. Lemberg, Nucl. Phys. **A145**, 129 (1970).
[102] N. I. Pyatov, S. I. Gabrakov, and D. I. Salamov, Yad. Fiz. **26**, 267 (1977) [Sov. J. Nucl. Phys. **26**, 139 (1977)].
[103] V. M. Mikhaĭlov, Yad. Fiz. **20**, 21 (1974) [Sov. J. Nucl. Phys. **20**, 11 (1975)].
[104] N. I. Pyatov, in: Materialy 10 Zimneĭ shkoly LIYaF (Proceedings of the Tenth Winter School of the Leningrad Institute of Nuclear Physics), Part 1, Leningrad (1975), p. 232.
[105] D. R. Bes and R. A. Broglia, Phys. Rev. C **3**, 2349 (1971); R. A. Broglia, D. R. Bes, and B. S. Nilsson, Phys. Lett. **50B**, 213 (1974).
[106] R. F. Casten, E. R. Flynn, I. D. Garrett *et al.*, Phys. Lett. **40B**, 333 (1972); D. R. Bes, R. A. Broglia, and B. Nilsson, Phys. Lett. **40B**, 338 (1972).
[107] I. Ragnarsson and R. A. Broglia, Nucl. Phys. **A263**, 315 (1976).
[108] A. I. Vdovin, D. Dambasuren, V. G. Solov'ev, and Ch. Stoyanov, Izv. Akad. Nauk SSSR Ser. Fiz. **40**, 2183 (1976); D. Dambasuren, Izv. Akad. Nauk SSSR Ser. Fiz. **41**, 1281 (1977).
[109] I. A. Mitropol'skiĭ, Yad. Fiz. **29**, 1466 (1979) [Sov. J. Nucl. Phys. **29**, 751 (1979)].
[110] I. A. Mitropol'skiĭ, Preprint No. 920 [in Russian], Leningrad Institute of Nuclear Physics, Leningrad (1984).
[111] B. S. Nielsen and M. E. Bunker, Nucl. Phys. **A245**, 376 (1975).
[112] N. K. Kuz'menko and V. M. Mikhaĭlov, Izv. Akad. Nauk SSSR Ser. Fiz. **44**, 942 (1980).
[113] B. L. Birbrair and I. A. Mitropol'skiĭ, Izv. Akad. Nauk SSSR Ser. Fiz. **45**, 23 (1981).
[114] S. T. Belyaev, in: Nuclear Structure, IAEA, Vienna (1968), p. 155.
[115] I. A. Mitropol'skiĭ, Preprint No. 680 [in Russian], Leningrad Institute of Nuclear Physics, Leningrad (1981); I. A. Mitropolsky, J. Phys. G **7**, 921 (1981).
[116] N. I. Pyatov, in: Materialy 8 Zimneĭ shkoly LIYaF (Proc. of the Eighth Winter School of the Leningrad Institute of Nuclear Physics), Part 2, Leningrad (1973), p. 282.
[117] N. K. Kuz'menko and V. M. Mikhaĭlov, Izv. Akad. Nauk SSSR Ser. Fiz. **43**, 2082 (1979); N. K. Kuz'menko and V. M. Mikhaĭlov, in: Tezisy dokladov 30-go Soveshchaniya po yadernoĭ spektroskopii i strukture atomnogo yadra (Abstracts of Papers at the 30th Symposium on Nuclear Spectroscopy and Nuclear Structure), Nauka, Leningrad (1980), p. 179.
[118] V. I. Abrosimov, Yad. Fiz. **31**, 348 (1980) [Sov. J. Nucl. Phys. **31**, 184 (1980)].
[119] O. Dumitrescu, Fiz. Elem. Chastits At. Yadra **10**, 377 (1979) [Sov. J. Part. Nucl. **10**, 147 (1979)].
[120] V. I. Abrosimov, Yad. Fiz. **32**, 961 (1980) [Sov. J. Nucl. Phys. **32**, 496 (1980)].
[121] I. S. Batkin, Yad. Fiz. **24**, 454 (1976); **28**, 1449 (1978) [Sov. J. Nucl. Phys. **24**, 235 (1976); *ibid.* **28**, 745 (1978)].
[122] I. A. Mitropol'skiĭ, Yad. Fiz. **33**, 1153 (1981) [Sov. J. Nucl. Phys. **33**, 611 (1981)].
[123] R. Abela, W. Kunold, L. M. Simons, and M. Schneider, Phys. Lett. **94B**, 331 (1980).

Translated by Julian B. Barbour